

Intuitive physical reasoning is not mediated by linguistic nor exclusively domain-general abstract representations

Hope Kean^{1,2}, Alexander Fung^{1,2}, RT Pramod^{1,2}, Jessica Chomik-Morales^{1,2}, Nancy Kanwisher^{1,2}, Evelina Fedorenko^{1,2}

¹Department of Brain & Cognitive Sciences, Massachusetts Institute of Technology

²McGovern Institute for Brain Research, Massachusetts Institute of Technology

Hope Kean: Conceptualization, Data Curation, Formal Analysis, Investigation, Methodology, Resources, Validation, Visualization, Writing -- Original Draft, Writing – Review & Editing
Alex Fung: Data Curation, Formal Analysis, Investigation, Methodology, Resources, Validation, Visualization, Writing – Review & Editing

RT Pramod: Data Curation, Investigation, Resources, Writing – Review & Editing

Jessica Chomik-Morales: Data Curation, Investigation, Resources, Writing – Review & Editing

Nancy Kanwisher: Methodology, Supervision, Writing – Review & Editing

Evelina Fedorenko: Conceptualization, Methodology, Project Administration, Supervision, Writing – Original Draft, Writing – Review & Editing

Acknowledgments:

We would like to acknowledge the Athinoula A. Martinos Imaging Center at the McGovern Institute for Brain Research at MIT, including the technical team—Steve Shannon and Atsushi Takahashi. We would also like to thank Kevin Smith, Anya Ivanova, Aryan Zoroufi, Josh Tenenbaum, Steve Piantadosi, and Dorothy Kean for invaluable comments and discussions on the manuscript, and Moshe Poliak for help with the statistical analyses. HK was supported by a graduate fellowship from the K. Lisa Yang Integrative Computational Neuroscience (ICoN) Center. EF was supported by research funds from the McGovern Institute for Brain Research, the Department of Brain and Cognitive Sciences, the Quest Initiative, and a grant from the Simons Foundation to the Simons Center for the Social Brain at MIT.

1
2
3
4
5
6
7

Intuitive physical reasoning is not mediated by linguistic nor exclusively domain-general abstract representations

Hope Kean^{1,2}, Alexander Fung^{1,2}, RT Pramod^{1,2}, Jessica Chomik-Morales^{1,2}, Nancy Kanwisher^{1,2}, Evelina Fedorenko^{1,2}

¹Department of Brain & Cognitive Sciences, Massachusetts Institute of Technology

²McGovern Institute for Brain Research, Massachusetts Institute of Technology

Hope Kean: Conceptualization, Data Curation, Formal Analysis, Investigation, Methodology, Resources, Validation, Visualization, Writing -- Original Draft, Writing – Review & Editing
Alex Fung: Data Curation, Formal Analysis, Investigation, Methodology, Resources, Validation, Visualization, Writing – Review & Editing

RT Pramod: Data Curation, Investigation, Resources, Writing – Review & Editing

Jessica Chomik-Morales: Data Curation, Investigation, Resources, Writing – Review & Editing

Nancy Kanwisher: Methodology, Supervision, Writing – Review & Editing

Evelina Fedorenko: Conceptualization, Methodology, Project Administration, Supervision, Writing – Original Draft, Writing – Review & Editing

Acknowledgments:

We would like to acknowledge the Athinoula A. Martinos Imaging Center at the McGovern Institute for Brain Research at MIT, including the technical team—Steve Shannon and Atsushi Takahashi. We would also like to thank Kevin Smith, Anya Ivanova, Aryan Zoroufi, Josh Tenenbaum, Steve Piantadosi, and Dorothy Kean for invaluable comments and discussions on the manuscript, and Moshe Poliak for help with the statistical analyses. HK was supported by a graduate fellowship from the K. Lisa Yang Integrative Computational Neuroscience (ICoN) Center. EF was supported by research funds from the McGovern Institute for Brain Research, the Department of Brain and Cognitive Sciences, the Quest Initiative, and a grant from the Simons Foundation to the Simons Center for the Social Brain at MIT.

1
2
3
4
5
6
Abstract
7
8
9
10
11
12
13
14
15
16
17
18
19
20
21
22
23
24
25
26
27
28
29
30
31
32
33
34
35
36
37
38
39
40
41
42
43
44
45
46
47
48
49
50
51
52
53
54
55
56
57
58
59
60
61
62
63
64
65

The ability to reason about the physical world is a critical tool in the human cognitive toolbox, but the nature of the representations that mediate physical reasoning remains debated. Here, we use fMRI to illuminate this question by investigating the relationship between the physical-reasoning system and two well-characterized systems: a) the domain-general Multiple Demand (MD) system, which supports abstract reasoning, including mathematical and logical reasoning, and b) the language system, which supports linguistic computations and has been hypothesized to mediate some forms of thought. We replicate prior findings of a network of frontal and parietal areas that are robustly engaged by physical reasoning and identify an additional physical-reasoning area in the left frontal cortex, which also houses components of the MD and language systems. Critically, direct comparisons with tasks that target the MD and the language systems reveal that the physical-reasoning system overlaps with the MD system, but is dissociable from it in fine-grained activation patterns, which replicates prior work. Moreover, the physical-reasoning system does not overlap with the language system. These results suggest that physical reasoning does not rely on linguistic representations, nor exclusively on the domain-general abstract reasoning that the MD system supports.

Introduction

The ability to reason about the physical world is essential to our everyday lives. According to one proposal, physical reasoning relies on a generative probabilistic model of physical causes and effects, similar to a video game's physics engine (Eberly, 2003; Battaglia et al., 2013). This "Intuitive Physics Engine" model includes a dictionary of representational primitives (e.g., objects, surfaces), knowledge of their physical properties, and of the constraints on object movement and inter-object or object-to-surface interactions, allowing for the representation of diverse physical events, including making predictions about how the world will change over time (Smith et al., 2013).

Where in the brain is this Intuitive Physics Engine implemented? Fischer et al. (2016) contrasted brain responses while participants made intuitive physical judgments versus performed a difficulty-matched color-judgment task on the same stimuli (**Fig. 2B**) and identified a set of frontal and parietal areas that respond more strongly during the physical-reasoning condition. In line with these areas' role in physical reasoning, subsequent work has established that they represent physical mass (Schwettmann et al., 2019) and stability (Pramod et al., 2022), and support forward prediction of physical events (Pramod et al., 2022; Fischer & Mahon, 2022).

What kind of representations mediate physical reasoning? One possibility is that physical reasoning draws on abstract domain-general representations that support other kinds of reasoning, like mathematical and logical reasoning. Indeed, the *topography* of the physical-reasoning system bears broad resemblance to the domain-general Multiple Demand (MD) system (Duncan, 2010, Fedorenko et al., 2013; Duncan et al., 2020), which is implicated in diverse goal-directed behaviors and supports several kinds of formal reasoning (Duncan & Owen 2000; Fox et al., 2005; Hampshire et al., 2011; Niendam et al., 2012; Fedorenko et al., 2013; Hearne et al., 2017; Amalric & Dehaene, 2019; Woolgar et al., 2018; Assem et al., 2020; Ivanova et al., 2020; Liu et al., 2020). In line with this possibility, past work has established that the representations in the physical-reasoning system are quite *abstract*: for example, representations of physical stability are invariant to the animacy of the object/entity (Pramod et al., 2022), representations of object mass are invariant to diverse aspects of the scene (Schwettmann et al., 2019), and representations of whether or not two objects make a contact are invariant to object and contact types (Pramod et al., under review). However, Fischer et al. (2016) found that the physical-reasoning areas are at least partially dissociable from the MD system. In line with this neural dissociation, physical reasoning appears to be cognitively separable from spatial cognition and general fluid intelligence, as revealed in a recent individual-differences behavioral investigation (Mitko & Fischer, 2024).

Another possibility is that physical reasoning draws on linguistic representations. Formal approaches to physical systems (such as the Physics Engine approach introduced above; Eberly, 2003) provide structured "languages" for representing dynamic, physical world states (for a related approach—situation calculus—see McCarthy & Hayes, 1969; Kowalski & Sergot, 1986; Pinto & Reiter, 1993). Such approaches emphasize the importance of rule-based changes to represent the dynamic physical world. Linguistic structures, including tense and aspect systems, robustly encode events and state changes (Partee, 1973, 1984; Moens, 1987; Moens & Steedman, 1988; Pulman, 1997; Grønn & von Stechow, 2016) and appear capable of subtly affecting the

encoding of the physical and social structure of visual events (Tversky & Kahneman, 1981; Gleitman, 1990; Skordos et al., 2020; Vurgun et al., 2022, 2024). These properties make linguistic structures well-suited as symbolic, rule-like representations of the physical world dynamics (Wong, Grand et al., 2023). The ability of large language models to develop an internal representation of the physical world—including spatial relations, object interactions, and causal structure—from text alone (Li et al., 2023; Nanda et al., 2023; Gurnee & Tegmark, 2023; Marks & Tegmark, 2024) further demonstrates the sufficiency of language for representing at least some aspects of the physical world. In addition, although some physical reasoning abilities are already present in infancy (Leslie & Keeble, 1987; Baillargeon et al., 1985, 1992; Spelke et al., 1992; Spelke, 2022), understanding of certain physical concepts, such as solidity and support, appear to exhibit a dip in performance during toddlerhood (e.g., Berthier et al., 2000; Hood et al., 2000, 2003). The causes of this dip are debated (e.g., Keen, 2003; Xu, 2019), but one possibility is that the development of linguistic abilities is transforming the early-emerging (“core”; Spelke, 2022) physical reasoning abilities (mediated by visual-perceptual representations) into more abstract and structured ones based on the linguistic encoding of information, and this process leads to temporary difficulties.

To shed further light on the representational format of intuitive physical reasoning, we first replicate Fischer et al.’s (2016) findings using a larger participant sample and identify an additional component of the physical-reasoning system in the left frontal cortex. The location of this new area provides additional motivation for examining overlap with the MD and language systems, both of which have left frontal components. In the critical analyses, we find that the physical-reasoning system overlaps with the MD system but is dissociable from it in the response profiles and fine-grained activation patterns, and it shows no overlap with the language system. Thus, physical reasoning—at least the type of reasoning examined here—does not recruit linguistic nor fully abstract domain-general representations, and plausibly relies on domain-specific knowledge structures.

Methods

Participants

Forty participants were recruited from MIT and the surrounding community. All participants were native speakers of English, had normal hearing and vision, and no history of language impairment. All but one participant were right-handed; the left-handed participant had a left-lateralized language system (as determined by the language localizer task described below), and was therefore included in all analyses (Willems et al., 2014). One (right-handed) participant had a right-lateralized language system and was excluded from the analysis of the language system’s responses to physical reasoning, leaving 39 participants for that analysis. All participants provided written informed consent in accordance with the requirements of MIT’s Committee on the Use of Humans as Experimental Subjects (COUHES) and were paid for their time.

Design

All participants completed the intuitive physics localizer task (Fischer et al., 2016) and a language localizer task (Fedorenko et al., 2010). Twenty-nine of the participants additionally

1
2
3
4 completed a spatial working memory task (from Fedorenko et al., 2011), which is commonly
5 used to localize the domain-general Multiple Demand system.
6

7
8 ***The intuitive physics localizer.*** This localizer, introduced in Fisher et al. (2016), included two
9 conditions in a blocked design. Participants viewed videos of unstable block towers made up of
10 yellow and blue blocks (**Fig. 2B**) located on a floor surface divided in the middle such that half
11 of the floor is red, and the other half is green. In the critical (Physics) condition, participants
12 judged whether—if the tower tumbles—more blocks would land on the red part of the floor or
13 the green part of the floor. In the control (Color) condition, participants judged whether the tower
14 contained more yellow or more blue blocks (**Fig. 2B**). The stimuli were visually identical
15 between the two conditions, and the tasks were matched for difficulty (Fisher et al., 2016). The
16 Physics > Color judgment contrast targets cognitive processes related to intuitive physical
17 reasoning. Each stimulus video presentation was 6 seconds long and the camera viewpoint
18 moved 360° completely circling the block tower. The towers consisted of between 13 and 39
19 blocks, and the number of blue vs. yellow blocks differed by one to six in every tower. Each
20 video was preceded by a question which appeared on the screen for 1 second cuing the type of
21 judgment the participant had to perform: either “where will it fall?” for the Physics task or “more
22 blue or yellow?” for the Color task. The videos were followed by a 2 second response period
23 with a blank screen, for a total trial duration of 9 seconds. Trials were grouped into blocks of 2
24 trials of the same condition (18 seconds total). Each scanning run consisted of 20 blocks (10 per
25 condition) and 3 blocks of a baseline blank screen (18 seconds each), for a total run duration of
26 414 seconds. Condition order was counterbalanced across runs. Each participant completed 2
27 runs.
28
29

30 ***The Multiple Demand system localizer.*** This spatial working memory task, introduced in
31 Fedorenko et al. (2011) and used in many subsequent studies as a localizer for the MD system
32 (Blank et al., 2014; Shashidhara et al., 2019, 2020, 2021, 2024; Diacheck, Blank, Siegelman et al.,
33 2020; Malik-Moraleda, Ayyash et al., 2022), included two conditions in a blocked design.
34 Participants had to keep track of spatial locations presented in a sequence (8 locations in the
35 Hard condition, 4 locations in the Easy condition) (**Fig. 2E**). The Hard > Easy contrast targets
36 cognitive processes broadly related to performing demanding tasks—what is often referred to by
37 an umbrella term ‘executive function processes’. Each trial consisted of a brief fixation cross
38 shown for 500 ms followed by 4 sequential flashes of unique locations within the 3 × 4 grid (1 s
39 per flash; two locations at a time in the Hard condition, one location at a time in the Easy
40 condition). Each trial ended with a two-alternative, forced-choice question (two sets of locations
41 were presented for up to 3.25 s, and participants had to choose the set of locations they just saw;
42 if they responded before 3.25 s elapsed, there was a blank screen for the remainder of the 3.25 s
43 period). Finally, participants were given feedback in the form of a green checkmark (correct
44 response) or a red cross (incorrect response or no response) shown for 250 ms. The total trial
45 duration was 8 seconds. Trials were grouped into blocks of 4 trials of the same condition (32
46 seconds total). Each scanning run consisted of 12 blocks (6 per condition) and 4 blocks of a
47 baseline fixation screen (16 seconds each), for a total run duration of 448 seconds. Condition
48 order was counterbalanced across runs. Each participant completed 2 runs.
49
50

51 Importantly, the Hard > Easy spatial working memory contrast generalizes to other contrasts of
52 more vs. less demanding conditions (e.g., Duncan & Owen, 2000; Fedorenko et al., 2013;
53
54
55
56
57
58
59
60
61
62
63
64
65

Hughdahl et al., 2015; Shashidara et al., 2019; Assem et al., 2020b), and a system that closely corresponds to the one activated by the MD system localizer emerges from task-free (resting state) data (e.g., Assem et al. 2020b; Braga et al., 2020; Du et al., 2024).

The language localizer. This localizer, introduced in Fedorenko et al. (2010) and used in many subsequent studies (e.g., Blank et al., 2016; Fedorenko et al., 2020; Hu, Small et al., 2022; Chen et al., 2023; Tuckute et al., 2024; Shain, Kean et al., 2024; the task is available for download from <https://www.evlab.mit.edu/resources>). Participants silently read sentences and lists of unconnected, pronounceable nonwords in a blocked design (**Fig. 3B**). The Sentences > Nonwords contrast targets cognitive processes related to high-level language comprehension, including understanding word meanings and combinatorial linguistic processing. Each stimulus (sentence or nonword list) was 6 seconds long and consisted of 12 words or nonwords presented one word/nonword at a time at the rate of 450 ms per word/nonword. The main task was attentive reading. Each stimulus was followed by a simple button-press task, which was included to maintain alertness. Trials were grouped into blocks of 3 trials of the same condition (18 seconds total). Each scanning run consisted of 16 blocks (8 per condition) and 5 blocks of a baseline blank screen (14s each), for a total run duration of 358 seconds. Condition order was counterbalanced across runs. Each participant completed 2 runs.

Importantly, the Sentences > Nonwords contrast generalizes across presentation modalities (e.g., reading vs. listening), tasks, stimuli within a language (e.g., sentences vs. passages), and diverse languages (e.g., Fedorenko et al., 2010; Scott et al., 2017; Ivanova et al., 2020; Chen et al., 2023; Malik-Moraleda, Ayyash et al., 2022; see Fedorenko et al., 2024 for a review). Moreover, a system that closely corresponds to the one activated by the language localizer emerges from task-free (resting state) data (Braga et al. 2020; Du et al., 2024). All brain regions identified by this contrast show sensitivity to lexico-semantic processing (e.g., stronger responses to real words than nonwords), combinatorial syntactic and semantic processing (e.g., stronger responses to sentences than to unstructured word lists, and sensitivity to syntactic complexity) (e.g. Fedorenko et al. 2010, 2016, 2020; Blank et al., 2016; Shain et al., 2022; Shain, Kean et al., 2024), and to sub-lexical regularities (Bozic et al., 2015; Regev et al. 2024).

Data acquisition, preprocessing, and first-level modeling

Data acquisition

Whole-brain structural and functional data were collected on a whole-body 3 Tesla Siemens Prisma/Prisma-fit scanner with a 32-channel head coil at the Athinoula A. Martinos Imaging Center at the McGovern Institute for Brain Research at MIT. T1-weighted anatomical images were collected in 176 axial slices with 1 mm isotropic voxels (repetition time (TR) = 2,530 ms; echo time (TE) = 3.57 ms (n=23 participants) or 3.48 ms (n=17 participants; a slightly different version of the sequence was used across the two subsets). For 23 participants, functional, BOLD data were acquired using a simultaneous multi-slice (SMS) imaging pulse sequence with a 90° flip angle using iPAT with an acceleration factor of 3; the following parameters were used: 66 2 mm thick slices acquired in an interleaved order (slice gap = 0 mm), with an in-plane resolution of 2 x 2 mm, FoV in the phase encoding (A >> P) direction 204 mm and matrix size 102 x 102 voxels, TR = 2,000 ms and TE = 35 ms. For the remaining 17 participants, functional, BOLD

1
2
3
4 data were acquired using a T2*-weighted echo planar imaging pulse sequence with a 90° flip
5 angle and using GRAPPA with an acceleration factor of 2; the following parameters were used:
6 31 4.4 mm thick near axial slices acquired in an interleaved order (with 10% distance factor),
7 with an in-plane resolution of 2.1 × 2.1 mm, FoV in the phase encoding (A >> P) direction 200
8 mm and matrix size 96 × 96 voxels, TR = 2,000 ms and TE = 30 ms. The first 10 s of each run
9 were excluded to allow for steady state magnetization.
10
11

12 ***Preprocessing***

13

14 fMRI data were preprocessed and analyzed using SPM12 (release 7487), CONN EvLab module
15 (release 19b), and other custom MATLAB scripts. Each participant's functional and structural
16 data were converted from DICOM to NIFTI format. All functional scans were coregistered and
17 resampled using B-spline interpolation to the first scan of the first session (Friston et al., 1995).
18 Potential outlier scans were identified from the resulting subject-motion estimates as well as
19 from BOLD signal indicators using default thresholds in CONN preprocessing pipeline (5
20 standard deviations above the mean in global BOLD signal change, or framewise displacement
21 values above 0.9 mm; Nieto-Castañón, 2020). Functional and structural data were independently
22 normalized into a common space (the Montreal Neurological Institute [MNI] template;
23 IXI549Space) using SPM12 unified segmentation and normalization procedure (Ashburner and
24 Friston 2005) with a reference functional image computed as the mean functional data after
25 realignment across all timepoints omitting outlier scans. The output data were resampled to a
26 common bounding box between MNI coordinates (-90, -126, -72) and (90, 90, 108), using 2
27 mm isotropic voxels and 4th order spline interpolation for the functional data, and 1 mm
28 isotropic voxels and trilinear interpolation for the structural data. Last, the functional data were
29 smoothed spatially using spatial convolution with a 4 mm FWHM Gaussian kernel.
30
31

32 ***First-level modeling***

33

34 For all experiments, effects were estimated using a general linear model (GLM) in which each
35 experimental condition was modeled with a boxcar function convolved with the canonical
36 hemodynamic response function (HRF) (fixation was modeled implicitly, such that all timepoints
37 that did not correspond to one of the conditions were assumed to correspond to a fixation
38 period). Temporal autocorrelations in the BOLD signal timeseries were accounted for by a
39 combination of high-pass filtering with a 128 s cutoff, and whitening using an AR (0.2) model
40 (first-order autoregressive model linearized around the coefficient $a = 0.2$) to approximate the
41 observed covariance of the functional data in the context of restricted maximum likelihood
42 estimation. In addition to experimental condition effects, the GLM design included first-order
43 temporal derivatives for each condition (included to model variability in the HRF delays), as
44 well as nuisance regressors to control for the effect of slow linear drifts, subject-motion
45 parameters, and potential outlier scans on the BOLD signal.
46
47

48 ***Second-level fMRI analyses***

49

50 The analyses were performed using the spm_ss toolbox (http://www.nitrc.org/projects/spm_ss),
51 which interfaces with SPM and the CONN toolbox (<https://www.nitrc.org/projects/conn>).
52
53

1
2
3
4 **fROI definition and response estimation**
5
6

7 *Definition of the physical-reasoning fROIs:* The initial Fischer et al. (2016) study included 12
8 participants; because our set of participants was larger ($n=40$) and probabilistic overlap maps
9 tend to show greater stability with more participants (e.g., Lipkin et al., 2022), we first
10 performed a group-constrained subject-specific (GSS) analysis (Fedorenko et al., 2010; Julian et
11 al., 2012) on our data in order to create a set of parcels that would be used for defining
12 individual-level fROIs. GSS is a whole-brain analysis that identifies spatially consistent (across
13 participants) areas of activation for some contrast of interest. To do so, we first thresholded the
14 individual t-maps for the Physics > Color contrast by selecting the 10% of most responsive
15 voxels across the brain. These maps were then binarized (selected voxels were turned into 1s and
16 the remaining voxels into 0s) and overlaid to create a probabilistic overlap map (summing the 1s
17 and 0s across participants in each voxel). After dividing the summed value in each voxel by the
18 number of participants (40, in this case), these values can be interpreted as the proportion of the
19 participants for whom that voxel belonged to the set of top 10% of most responsive voxels (Fig.
20 1A). This probabilistic overlap map was then thresholded, such that voxels with values of 0.1 or
21 lower were removed, and a watershed algorithm was used to segment the map into discrete
22 regions (parcels).
23
24

25 The parcels were evaluated on two criteria. First, each parcel was intersected with the individual
26 binarized activation maps to calculate how many participants have task-responsive voxels within
27 the parcel boundaries. Parcels where 24/40 (60%) or more of the participants had task-responsive
28 voxels were included (Fig. 1B). And second, we evaluated the replicability of the Physics >
29 Color contrast. To do so, we used an across-runs cross-validation approach to ensure
30 independence between the data used to define the fROIs and to estimate the effects (e.g.,
31 Kriegeskorte et al., 2011; Nieto-Castañón & Fedorenko, 2012). In particular, we used run 1 of
32 the task to define the functional regions of interest (fROIs) (as the top 10% of most responsive
33 voxels within each parcel, based on the t-values for the Physics > Color contrast; note that this
34 approach ensures that a fROI is defined in every participant, cf. a fixed statistical threshold
35 approach, for which some participants may not have any significant voxels in a given parcel) and
36 run 2 to estimate the responses; then we used run 2 to define the fROIs and run 1 to estimate the
37 responses; finally, we averaged these estimates to obtain a single estimate per participant per
38 parcel. Parcels where the Physics > Color contrast reliably differed from zero were included in
39 the critical analyses.
40
41

42 To examine the responses in the physics fROIs to the conditions of other tasks, the fROIs were
43 defined using the data from both runs of the physics localizer.
44
45

46 *Definition of the MD fROIs:* Each individual map for the Hard > Easy spatial working memory
47 contrast from the MD localizer was intersected with a set of 20 parcels (10 in each hemisphere).
48 These parcels (available at <https://www.evlab.mit.edu/resources>) were derived from a
49 probabilistic activation overlap map for the same contrast in a large set of independent
50 participants ($n=197$) and covered the frontal and parietal components of the MD system
51 bilaterally (Duncan 2010; Fedorenko et al., 2013). Within each parcel, a participant-specific MD
52 fROI was defined as the top 10% of voxels with the highest t-values for the localizer contrast. To
53 estimate the response in the MD fROIs to the conditions of the MD localizer, the same cross-
54
55

validation procedure was used as described above. As expected, the MD fROIs showed a robust Hard > Easy spatial working memory effect ($p_s < 0.001$, $|d|_s > 1.84$).

Definition of the language fROIs: Each individual map for the Sentences > Nonwords contrast from the language localizer was intersected with a set of 5 parcels. These parcels (available at <https://www.evlab.mit.edu/resources>) were derived from a probabilistic activation overlap map for the same contrast in a large set of independent participants ($n=220$) and covered the fronto-temporal language system in the left hemisphere (Fedorenko et al., 2024). Within each parcel, a participant-specific language fROI was defined as the top 10% of voxels with the highest t-values for the localizer contrast. To estimate the response in the language fROIs to the conditions of the language localizer, the same cross-validation procedure was used as described above, to ensure independence. As expected, the language fROIs showed a robust Sentences > Nonwords effect ($p_s < 0.001$, $|d|_s > 2.05$; here and elsewhere, p-values are corrected for the number of fROIs using the false discovery rate (FDR) correction (Benjamini and Yekutieli, 2001)).

Statistical analyses of fROI response profiles

All analyses were performed with linear mixed-effects models using the “lme4” package in R (version 1.1.26; Bates et al., 2015) with p value approximation performed by the “lmerTest” package (version 3.1.3; Kuznetsova et al., 2017) and effect sizes (Cohen’s d) estimated by the “EMAtools” package (version 0.1.3; Kleiman, 2017).

Past work on the physical-reasoning, language, and MD systems has established that different regions within each system show functionally similar responses. However, to allow for potential differences in the degree of inter-system overlap in different parts of the brain, we chose to differentiate among the regions in each system. For the physical-reasoning and MD systems, we grouped regions into a few sets based on anatomy. In particular, for the physical-reasoning system, we grouped fROIs into eight sets: left hemisphere (LH) anterior frontal, LH posterior frontal, LH and right hemisphere (RH) superior frontal, LH and RH parietal, and LH and RH temporal-parietal (Fig. 2C). For the MD system, we also grouped fROIs into eight sets: LH and RH medial-superior frontal, LH and RH precentral + middle frontal, LH and RH insular, and LH and RH parietal (Fig. 2F; see also SI 2-3 for the results on the individual fROIs for the physical-reasoning and the MD systems). For the language system, we examined the five fROIs separately.

First, to examine responses to each contrast in each system, we fit a linear mixed-effect regression model for each fROI (for the language system) or fROI group (for the physical-reasoning and MD systems) predicting the level of BOLD response from condition, with random intercepts for fROIs (when groups consisted of multiple fROIs) and participants:

$$\text{BOLD} \sim \text{Condition} + (1 | \text{fROI}) + (1 | \text{Participant})$$

For comparisons between systems for a given contrast (e.g., asking whether the Physics > Color contrast is significantly larger in the physical-reasoning system compared to the MD system), we fit a linear mixed-effect regression model predicting the level of BOLD response from condition, system, and their interaction, with random intercepts for fROIs and participants:

1
2
3
4
5 *BOLD ~ Condition * System + (I | fROI) + (I | Participant)*
6
7

8 In a similar fashion, for comparisons between tasks within a system (e.g., asking whether in the
9 physical-reasoning system the Physics > Color contrast is significantly larger than the Hard >
10 Easy contrast from the spatial working memory task), we fit a linear mixed-effect regression
11 model predicting the level of BOLD response from condition (critical vs. control), task (e.g.,
12 physics vs. spatial WM), and their interaction, with random intercepts for fROIs and participants:
13
14

15 *BOLD ~ Condition * Task + (I | fROI) + (I | Participant)*
16
17

18 ***Whole-brain multivariate correlation analyses*** 19

20 Given that, as will be discussed below, the inter-system overlap analyses via univariate fROI
21 response profiles revealed some overlap between the physical-reasoning and the MD systems,
22 we asked whether the activation patterns for the Physics > Color and Hard > Easy Spatial WM
23 contrasts may be dissociable in their fine-grained spatial topographies, similar to an analysis
24 reported in Fischer et al. (2016). To do so, we first created probabilistic activation overlap atlases
25 for each contrast. This procedure is described for the Physics > Color contrast in “fROI
26 definition and response estimation”; for the Hard > Easy contrast, we used the probabilistic atlas
27 created from n=691 participants (Lipkin et al., 2022; doi.org/10.6084/m9.figshare.22306348).
28 We then computed a correlation between each individual map for the Physics > Color contrast
29 (n=40 participants) and each of the two atlases, and between each individual map for the Hard >
30 Easy contrast (n=29 participants) and each atlas. The distributions of these correlations were
31 compared via independent-samples t-tests, to see whether the maps for the Physics > Color
32 contrast are more similar to the physical-reasoning system atlas versus the MD system atlas, and
33 whether the maps for the Hard > Easy spatial working memory contrast are more similar to the
34 MD system atlas versus the physical-reasoning system atlas (**Figure 2G**).
35
36
37
38

39 **Results** 40

41 ***1. Replication and extension of prior findings on the physical-reasoning system (Fischer et al., 42 2016): A set of bilateral frontal, temporal, and parietal areas support physical reasoning.*** 43

44
45 Using an fMRI localizer paradigm introduced in Fischer et al. (2016), we identified a set of brain
46 areas engaged during physical reasoning. The paradigm is based on a contrast of judgments
47 about physical stability of rotating block towers (the critical condition) vs. about the color
48 composition of the same towers (**Figure 2B**). The critical condition requires participants to rely
49 on their intuitions about the tower’s center of gravity to decide whether more blocks would fall
50 on one or the other half of the floor surface. A whole-brain GSS analysis (see Methods)
51 identified 21 parcels corresponding to areas of spatially consistent (across participants) activation
52 for the Physics > Color contrast (**Figure 1A-C**). Based on the combination of two criteria—
53 presence in 60% or more of the participants and replicability of the Physics > Color effect across
54 runs—19 of the 21 parcels were selected for the critical analyses (**Figure 1C**).
55
56
57
58
59
60
61
62
63
64
65

The topography of these parcels—spanning frontal and parietal cortices bilaterally—closely mirrors Fischer et al.’s (2016) findings (Figure 2B in the 2016 paper, included as an inset in **Figure 1D**) and a subsequent study using the same localizer paradigm (Pramod et al., 2022). However, in our data, an additional area in the left anterior frontal lobe emerged, which passed our inclusion criteria. This area was likely missed in the earlier studies because of its small size; smaller areas become easier to detect with larger samples of participants (e.g., Lipkin et al., 2022). The fROIs defined within these parcels all show a robust Physics > Color effect, as estimated using an across-runs cross-validation approach (p_s for all fROI groups <0.001 ; **Figure 2A, C; Table 1A**).

Note also that both Fischer et al. (2016) and Pramod et al. (2022) exclude a subset of the parcels from consideration—the bilateral temporo-parietal and the LH posterior frontal ones—because they failed to pass an additional test (see **Figure 1D** for the comparisons of the parcels). In particular, in addition to the physical stability localizer, Fischer et al. (2016) had participants perform a task where they were asked to make physical vs. social judgments about simple moving geometric stimuli (two colored dots). Only the bilateral superior frontal and parietal regions showed a physical > social effect in that task. In our analyses, we examine the full set of regions for completeness, but we also report a version of the critical analyses where we only include the bilateral superior frontal and parietal regions for ease of comparison with prior work (see the rows referring to the Fischer subset in **Tables 1A-B, 4A-B**, and **Supp. Tables 1A-B**).

2. The physical-reasoning system is at least partially dissociable from the Multiple Demand system.

Next, we examined the relationship between the physical-reasoning system and the Multiple Demand (MD) system, whose topography broadly resembles the physical-reasoning system (**Figure 1E**). For this analysis, we used the subset of 29 participants, who performed an MD system localizer (**Figure 2E**). We performed two types of analyses to assess inter-system overlap.

First, we examined the response profiles in the two sets of fROIs, starting with the MD fROIs. Replicating much prior work (e.g., Fedorenko et al., 2013; Assem et al., 2020a,b), the MD fROIs show a robust Hard > Easy effect for the spatial working memory task (used as the localizer), as estimated using an across-runs cross-validation approach (p_s for all fROI groups <0.001 ; **Figure 2D, F; Table 2A**). Critically, several of the MD fROI groups also show a positive (and a few—significant) Physics > Color contrast (**Table 2B**; see **Supp. Table 3A** for the responses of the MD fROIs to all contrasts, and **Supp. Table 3B** for comparisons across tasks). However, the effect is overall small (**Figure 2D, F**) and significantly smaller than in the physical-reasoning system, as supported by a reliable condition-by-system interaction ($p < 0.001$; **Table 4A**). That said, in the flip-side analysis, where we examined the responses of the physical-reasoning fROIs to the spatial working memory task, we found strong responses and significant Hard > Easy effects in six of the eight fROI groups (**Supp. Figure 3**; see **Supp. Table 1A** for the responses of the physical-reasoning fROIs to all contrasts, and **Supp. Table 1B** for comparisons across tasks), although the size of the Hard > Easy effect is significantly smaller than in the MD system, as supported by a reliable condition-by-system interaction ($p < 0.001$; **Table 4B**). It is interesting to note that the left anterior frontal physical-reasoning fROI, which did not emerge in the Fischer et

al. (2016) study, shows the most selective profile relative to the spatial working memory task, with the response to the hard spatial memory condition being no higher than the response to the control, Color condition of the physical-reasoning localizer (**Supp. Figure 3**); in all other physical reasoning fROIs, the response to the hard spatial working memory condition is as high or higher than the critical, Physics condition.

Given this partial overlap, in the second analysis, we examined fine-grained spatial topographies to see if they show a dissociation (see Fisher et al., 2016, for a similar analysis). We found that the individual activation maps for the physical-reasoning task show a stronger correlation with the probabilistic atlas for the physical-reasoning system (mean $r=0.33$, SEM=0.02) compared to the MD system atlas ($r=0.08$, SEM=0.03; $t=6.928$; $p<0.001$). In contrast, the individual activation maps for the spatial working memory task show a stronger correlation with the probabilistic atlas for the MD system (mean $r=0.43$, SEM=0.03) compared to the physical-reasoning system atlas ($r=0.08$, SEM=0.03; $t=5.544$; $p<0.001$). Thus, although the two systems overlap spatially, the fine-grained activation patterns are robustly distinct (**Figure 2G**).

3. The physical-reasoning system does not overlap with the language system.

Finally and critically, we examined the relationship between the physical-reasoning system and the language-selective system—a relationship that has not been previously explored. We first examined the responses in the language fROIs to the physical-reasoning task. Replicating much prior work (see Fedorenko et al., 2024 for a review), the language regions show a robust Sentences > Nonwords effect, as estimated using an across-runs cross-validation approach (ps for all fROIs <0.001 ; **Figure 3A, C**; **Table 3A**; see **Supp. Table 2A** for the responses of the language fROIs to all contrasts, and **Supp. Table 2B** for comparisons across tasks). Critically, however, these regions do not respond to the physical-reasoning task (**Figure 3C; Table 3B**). The effect does not reach significance at the system level; it does reach significance in two fROIs, but a) the effect is small, b) the responses to both the Physics and the Color conditions are close to the fixation baseline, and c) the response to the Physics condition is substantially below the control, Nonwords, condition of the language localizer. Similarly, in the flip-side analysis, where we examined the responses of the physical-reasoning fROIs to the language task, we found that they do not respond to the Sentences > Nonwords contrast; in fact, similar to what has been previously reported for the MD network (e.g., Fedorenko et al., 2012, 2013), most of the physical-reasoning fROI groups respond more strongly to the Nonwords compared to the Sentences condition, and some reliably so (**Figure 4A, C; Table 1B**).

In addition to examining the relationship of the physical-reasoning system to the MD system and the language system, we examined its relationship to another high-level reasoning system: the social reasoning or ‘Theory of Mind’ network (e.g., Saxe & Kanwisher, 2003); some components of this system fall in broadly similar areas as the physical-reasoning brain areas (**Supp. Figure 1**). For the 21 participants who completed a ‘Theory of Mind’ localizer task (Saxe & Kanwisher, 2003; Dodel-Feder et al., 2011), we performed similar overlap analyses as for the other systems and found almost no overlap (**Supp. Figure 1; Supp. Tables 4A, B**).

Discussion

We here examined the physical-reasoning system, which was originally identified by Fischer et al. (2016; see also Schwettmann et al., 2018; Pramod et al., 2022), and its relationship with other known cognitive systems in an effort to illuminate the representations that may mediate intuitive physical reasoning. We replicated Fischer et al.'s original findings of a set of frontal and parietal brain areas that respond more strongly during a physical reasoning task (making physical stability judgments about block towers) than a difficulty-matched color-judgment task on the same stimuli, although we found an additional area in the anterior left frontal lobe. We found that the physical-reasoning system overlaps with the domain-general Multiple Demand (MD) system (Duncan, 2010), which has been implicated in executive control and in some forms of reasoning (e.g., Duncan & Owen 2000; Fox et al., 2005; Hampshire et al., 2011; Niendam et al., 2012; Fedorenko et al., 2013; Hearne et al., 2017; Amalric & Dehaene, 2019; Woolgar et al., 2019; Assem et al., 2020; Ivanova et al., 2020; Liu et al., 2020). However, in line with an analysis reported in Fischer et al. (2016), we found a dissociation in the fine-grained patterns of activation (see Pramod et al., in prep. for a more in-depth exploration of the relationship between the physical-reasoning system and the MD system). Moreover, the newly discovered left anterior frontal area shows clear selectivity relative to the spatial working memory task in its univariate response profile. Critically, we found that the physical-reasoning system does not overlap with the language-selective system: the response in the language areas during physical reasoning is close to the low-level baseline, and the physical-reasoning areas show a stronger response to the nonword-list condition compared to the sentence condition—the opposite of the response in the language system. Below we discuss the implications of these findings for our understanding of physical reasoning and the general structure of human cognition.

First, this work sheds light on the mental representations that undergird our processing of the physical world around us. Here, we replicate a past finding that the physical-reasoning system is at least partially dissociable from the domain-general MD system, which rules out the possibility that we represent the physical world using the kind of abstract representations that enable diverse goal-directed behaviors, novel problem solving, and mathematical reasoning (Duncan, 2010; Duncan et al., 2020; Amalric & Dehaene, 2019; Woolgar et al., 2019; Ivanova et al., 2020; Liu et al., 2020). The lack of overlap with the language network further rules out the hypothesis that our representations of the physical world are linguistic in nature, in spite of the fact that they may be symbolic (e.g., Battaglia et al., 2013; Smith et al., 2013). The physical-reasoning system may be a unique system in that it shares perceptual grounding with e.g., high-level visual areas (such as the fusiform face area or the parahippocampal place area; Kanwisher et al., 1997; Epstein et al., 2001) but, at the same time, shows selectivity for particular types of abstract content (e.g., representations of an object's mass or stability; Schwettmann et al., 2019; Pramod et al., 2022), which is characteristic of high-level systems of reasoning, such as the Theory of Mind system (Saxe & Kanwisher, 2003) or the MD system (Duncan, 2010). An interesting question to explore in future work is whether the components of the physical-reasoning system that are located in closer proximity to the MD system encode more abstract features of physical events. Based on the spatial proximity to—and partial overlap with—the MD system, one could also speculate that the two systems were one and the same earlier in the mammalian evolutionary history, as has been hypothesized for some spatially adjacent large-scale networks (e.g., DiNicola & Buckner, 2022; Deen & Freiwald, 2022); in particular, perhaps the MD system split off from the physical-reasoning system with the expansion of the association cortex (Buckner & Krienen, 2013), which

allowed for a greater degree of abstraction beyond the representations of the local physical environment.

Second, this study adds to the growing body of evidence suggesting that the language system is highly specialized for linguistic computations and does not support non-linguistic cognition. The language areas are not engaged when individuals perform diverse forms of reasoning (e.g., Monti et al., 2009, 2012; Fedorenko et al., 2011; Ivanova et al., 2020), and some individuals with severe linguistic deficits (aphasia) retain their ability to think (Varley & Siegal, 2000; Varley et al., 2005; for reviews see Fedorenko & Varley, 2016; Fedorenko et al., 2024a,b). Our study adds intuitive physical reasoning to the list of diverse types of reasoning that do not engage linguistic processing. However, it remains an open question whether physical reasoning that involves more abstract or formal concepts might engage the language system (or other high-level cognitive systems, such as the MD or the ToM system).

Third, our study contributes to the understanding of the ontology of cognition/thought. Prior research has identified a specialized system for thinking about others' mental states—sometimes referred to as theory of mind (ToM) or mentalizing (e.g., Saxe & Kanwisher, 2003; Saxe & Powell, 2006). Fischer et al. (2016) reported a system for intuitive physical reasoning (Fischer et al., 2016)—a finding that we replicate. By demonstrating that the physical-reasoning system is distinct from the ToM system and at least partially, from the domain-general MD system (see also Pramod et al., in prep.), we provide additional evidence that human cognition relies on multiple specialized systems rather than a single, general-purpose reasoning system. This distinction is further supported by behavioral individual-differences studies. For example, Mitko and Fischer (2024) observed a dissociation between performance on intuitive physical reasoning tasks and tasks tapping spatial cognition. These dissociations beg the question of what other kinds of reasoning may be supported by specialized systems. Developmental work on core knowledge systems (Spelke & Kinzler, 2007) can provide inspiration for additional domain-specific reasoning systems built out of early-emerging conceptual primitives.

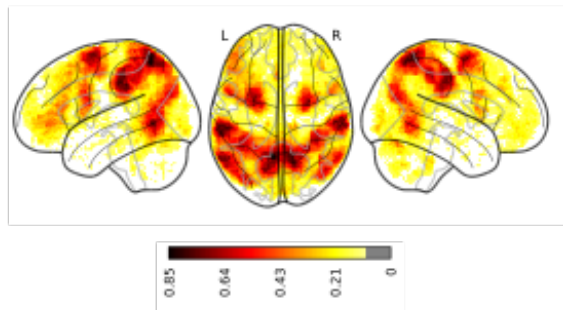
Finally, our findings highlight the functional heterogeneity of the left frontal lobe. Contra unified accounts of frontal lobe function (Cohen et al., 1996; Miller & Cohen, 2000; Duncan et al., 1996, 2000; Dosenbach et al., 2006; Cole & Schneider, 2007), evidence exists of both structural (e.g., Amunts et al., 2010) and functional distinctions among nearby areas in the frontal cortex. With respect to functional dissociations, the left frontal lobe in humans has been shown to house components of the language and the MD systems (Fedorenko et al., 2012, 2013; see Fedorenko & Blank, 2020 for a review), the articulatory motor-planning area (Hillis et al., 2004; Flinker et al., 2015; Long et al., 2015; Basilakos et al., 2018; Wolna et al., 2024)—the area originally discovered by Broca; Broca, 1861), components of the Theory of Mind network and the episodic default network (e.g., DiNicola et al., 2024; Du et al., 2024), and perhaps areas specialized for aspects of logical reasoning (Coetzee & Monti, 2018; Kean et al., 2024) and causal reasoning (Pramod et al., 2024). Fischer et al.'s (2016) results further established the existence of physical-reasoning areas in the frontal cortex that are at least partially dissociable from the MD system. We replicate these findings and identify an additional component of the physical-reasoning system in the anterior left frontal lobe. As new selectivities continue to emerge, understanding the organizational principles of the frontal cortex becomes increasingly important. Although it remains possible that some computations are shared among all of these distinct areas, any

1
2
3
4 account that spans these established functional boundaries would need to explain this
5 heterogeneity of response and functional connectivity profiles (see Xu et al., 2022 for evidence
6 that even in non-human primates, the frontal lobes are highly functionally heterogeneous, with
7 different areas exhibiting distinct patterns of connections to posterior brain areas; and see
8 Mansouri et al. 2006, 2015, 2017, 2022, 2024 for evidence that lesions to different frontal areas
9 in non-human primates lead to distinct kinds of behavioral deficits).
10
11

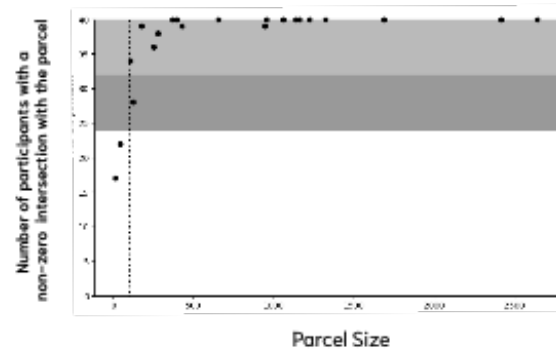
12 Overall, our study contributes to the understanding of the neural architecture underlying high-
13 level cognitive functions. We provide evidence that intuitive physical reasoning is mediated by
14 specialized, domain-specific representations that are distinct from both linguistic and domain-
15 general abstract representations. The existence of specialized systems for different types of
16 reasoning suggests that the modular nature of the human mind and brain extends beyond the
17 perceptual domain (e.g., Kanwisher, 2010) and highlights the need for further research into the
18 ontology of human thought, as well as into how these different systems work together to enable
19 complex thought and behavior.
20
21

22
23
24
25
26
27
28
29
30
31
32
33
34
35
36
37
38
39
40
41
42
43
44
45
46
47
48
49
50
51
52
53
54
55
56
57
58
59
60
61
62
63
64
65

A. Physical-reasoning Atlas



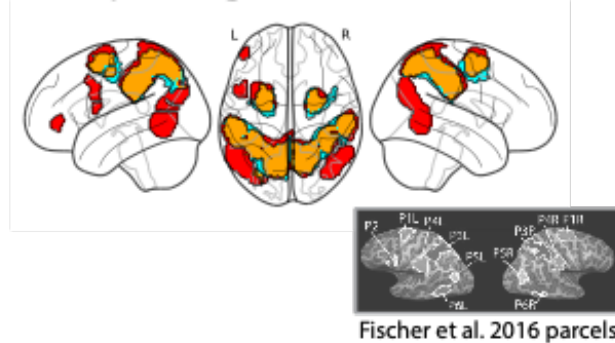
B.



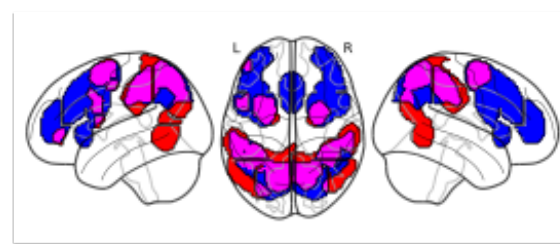
C. Physical-reasoning parcels



D. Overlap with the physical-reasoning parcels from Pramod et al. (2022) (overlap=orange)



E. Overlap with the MD system parcels (overlap=pink)



F. Overlap with the Language system parcels (overlap=yellow)

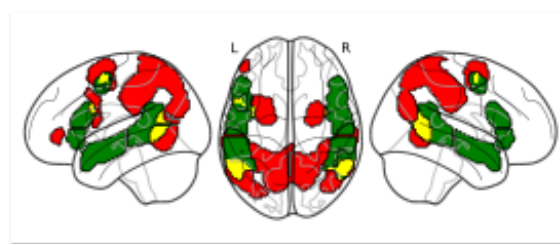


Figure 1. The physical-reasoning system and its broad anatomical overlap with other systems. A. A probabilistic atlas for the physical-reasoning system based on n=40 participants in the current study. This atlas is derived from individual activation maps for the Physics > Color contrast, where in each individual, we selected the top 10% of most reliable voxels. Areas with darker colors (orange and red) correspond to areas where a higher proportion of participants showed voxel-level overlap. B. The relationship between the size of the parcels (for the full set of 21 parcels that resulted from the GSS analysis) and the number of participants that have a non-zero intersection with the parcel (i.e., at least 1 voxel within the borders of the parcel was selected as the top 10% of Physics > Color voxels across the brain). The parcels (n=18) that fall within the light gray area have a nonzero intersection with 32 or more of the 40 participants (80% or more);

the parcel that falls within the dark gray area has a nonzero intersection with 24 or more of the participants (60% or more). C. The 21 parcels that emerged from the GSS analysis. Two parcels that did not meet our selection criteria are shown in gray. D. Overlap between our physical-reasoning parcels (red) and those from Pramod et al. (2022) (light blue). The overlap is shown in orange. Note that Pramod et al.'s set excludes the temporo-parietal parcels bilaterally and the left posterior frontal parcels (see text for details). Otherwise, there is good concordance between the two sets, except that our analysis reveals an additional area in the anterior left frontal lobe. The inset shows the parcels from the original Fischer et al. (2016) study. E. Overlap between our physical-reasoning parcels (red) and the Multiple Demand parcels (blue; these parcels were derived from a GSS analysis on a dataset of 197 participants; Lipkin et al., 2022). The two sets of parcels show overlap in both frontal and parietal areas. F. Overlap between our physical-reasoning parcels (red) and the language parcels (green; these parcels were derived from a GSS analysis on a dataset of 220 participants). The two sets of parcels show overlap in both frontal and temporal areas.

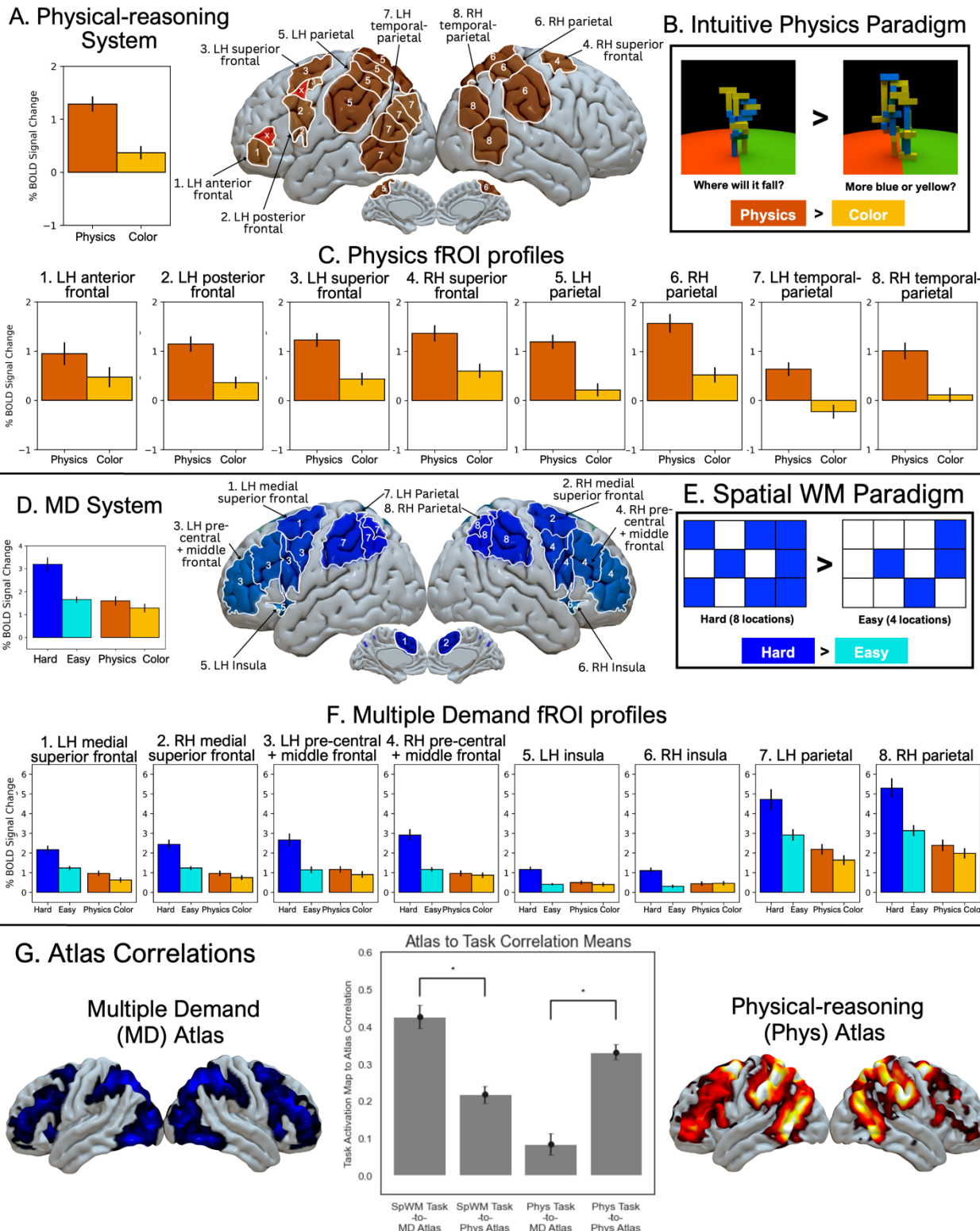
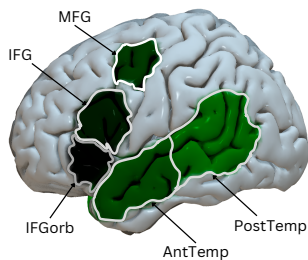
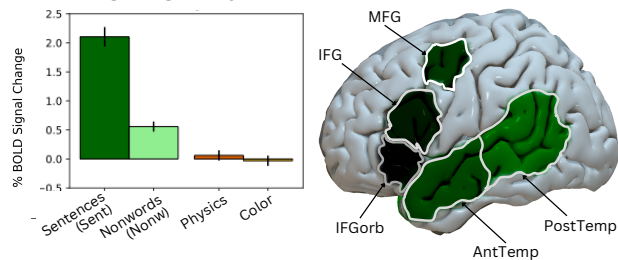


Figure 2. The physical-reasoning system and its relationship with the Multiple Demand system

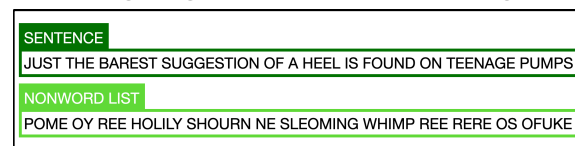
A. The response in the physical-reasoning fROIs to the physical-reasoning localizer conditions (Physics, Color), averaged across the fROIs; and the physical-reasoning system parcels (excluding parcels 20, 21, shown in red; see [Methods](#)). **B.** The physical-reasoning localizer. During the critical (Physics)

condition, participants answered “where will it fall?” by judging whether the block tower would fall towards the green or red side of the floor; during the control (Color) condition, participants answered “more blue or yellow?” by judging whether the block tower consisted of more yellow or blue blocks (see [Methods](#) for details). **C.** The response in the physical-reasoning fROIs, broken down by fROI group, to the physical-reasoning localizer conditions (Physics, Color). We observe a strong Physics>Color effect in all fROI groups (**Table 1A**). **D.** The response in the MD system fROIs to the spatial working memory MD localizer and physical-reasoning localizer conditions (Hard, Easy, Physics, Color), averaged across the fROIs; and the MD system parcels. **E.** The spatial working memory MD localizer. Participants were tasked with remembering four sequential flashes of unique locations with a 3x4 grid. During the Hard condition, each flash consisted of a pair of locations, while during the Easy condition, each flash consisted of a single location (see [Methods](#) for details). **F.** The response in the MD system fROIs, broken down by fROI group, to the MD localizer and physical-reasoning localizer conditions (Hard, Easy, Physics, Color). We observe a strong Hard>Easy effect in all fROI groups (**Table 2A**). **G.** Pearson correlation between physical-reasoning and MD system atlases to the physical-reasoning localizer and spatial working memory MD localizer task contrasts (Physics>Color, Hard>Easy). Here and elsewhere, error bars show standard error of the mean across participants.

A. Language System



B. Language Localizer Paradigm



C. Individual language fROIs

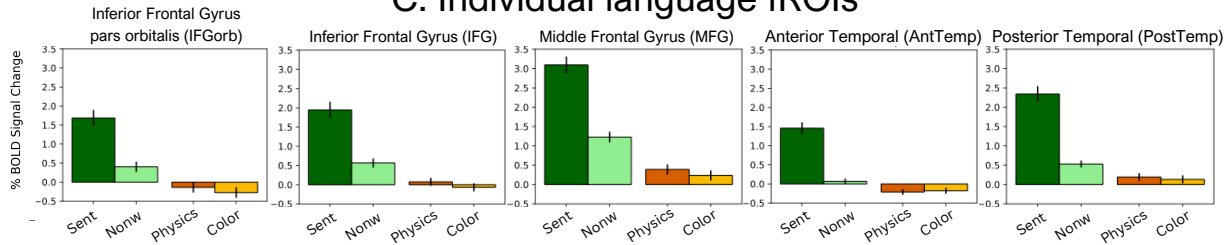


Figure 3. The language system and its relationship to physical-reasoning. **A.** The response in the language system fROIs to the language localizer and to the physical-reasoning localizer conditions (Sentences, Nonwords, Physics, Color), averaged across the fROIs; and the language system parcels. **B.** The language localizer. During Sentences trials, participants viewed complete sentences one word at a time. During Nonwords trials, participants viewed nonword lists (see [Methods](#) for details). **C.** The response to the language localizer and physical-reasoning localizer conditions (Sentences, Nonwords, Physics, Color), broken down by individual fROI within each system. We observe a strong Sentences>Nonwords effect in all fROIs (**Table 3A**).

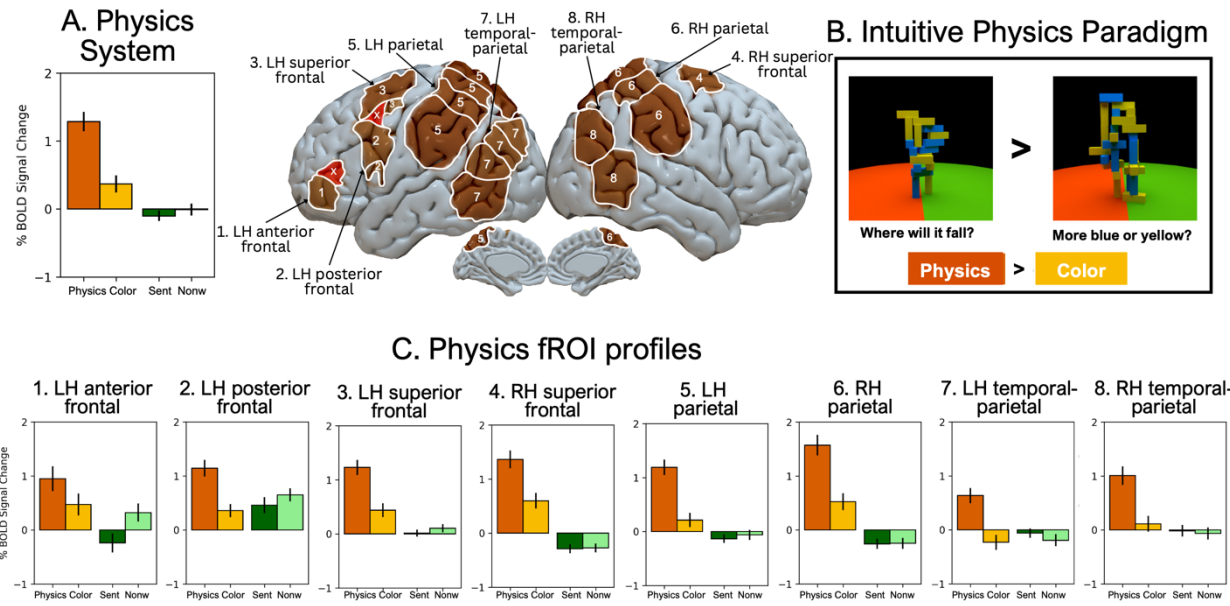


Figure 4. The physical-reasoning system and its relationship language processing. **A.** The response in the physical-reasoning system fROIs to the physical-reasoning localizer and language localizer conditions (Physics, Color, Sentences, Nonwords), averaged across the fROIs; and a display of the physical-reasoning system parcels (excluded parcels 20 and 21 shown in red; see [Methods](#)). **B.** The language localizer. During Sentences trials, participants viewed complete sentences one word at a time. During Nonwords trials, participants viewed nonword lists (see [Methods](#) for details). **C.** The response to the physical-reasoning localizer and language localizer conditions (Physics, Color, Sentences, Nonwords), broken down by individual fROI group. We observe a strong Physics>Color effect in all fROI groups (**Table 1A**) and no positive Sentences>Nonwords effect in any fROI group (**Table 1B**).

Task	Type	Beta	SEM	t	p
Phys	System	0.886829961	0.042281108	20.97461518	< 0.001
Phys	System_CoreRegions	1.01288101	0.05558128	18.2234187	< 0.001
Phys	Group Phys_LH_ant_front	0.476769375	0.128333818	3.71507201	< 0.001
Phys	Group Phys_LH_post_front	0.784105	0.106551568	7.358925023	< 0.001
Phys	Group Phys_LH_sup_front	0.78933915	0.097375336	8.10615074	< 0.001
Phys	Group Phys_RH_sup_front	0.76371005	0.097112027	7.864216993	< 0.001
Phys	Group Phys_LH_parietal	1.085572613	0.096197281	11.28485751	< 0.001
Phys	Group Phys_RH_parietal	1.148043775	0.110693093	10.37141292	< 0.001
Phys	Group Phys_LH_temp_par	0.865920931	0.086946198	9.959273049	< 0.001
Phys	Group Phys_RH_temp_par	0.894639563	0.116689265	7.666854055	< 0.001

Table 1A. The responses of the physical-reasoning system to the Physics > Color contrast. This table reports the beta estimates, standard errors of the mean, t-values, and p-values from a linear mixed-effects model (see [Methods](#)). We first report the effects for the system as a whole, for the core regions that Fischer et al. (2016) and subsequent studies focused on (for ease of comparisons with those earlier studies), and then for each fROI group separately. For the fROI groups, we report uncorrected p-values, but we mark the values that survive the Bonferroni correction for the number of fROI groups (n=9: 8 groups and the system as a whole) in **bold font**.

Task	Type	Beta	SEM	t	p
Lang	System	-0.075711934	0.039322957	-1.925387621	0.0544
Lang	System_CoreRegions	-0.1465097	0.03765454	-3.8908903	< 0.001
Lang	Group Phys_LH_ant_front	-0.560139487	0.137039845	-4.0874206	< 0.001
Lang	Group Phys_LH_post_front	-0.189940833	0.117520655	-1.616233612	0.1090
Lang	Group Phys_LH_sup_front	-0.092001038	0.072940223	-1.261321044	0.2100
Lang	Group Phys_RH_sup_front	-0.017213538	0.044340009	-0.388216845	0.7000
Lang	Group Phys_LH_parietal	-0.279767731	0.075482864	-3.706374084	< 0.001
Lang	Group Phys_RH_parietal	-0.048270043	0.069019309	-0.699370127	0.4850
Lang	Group Phys_LH_temp_par	0.133383455	0.107004067	1.246526968	0.2140
Lang	Group Phys_RH_temp_par	0.048880705	0.111723531	0.437514861	0.6630

Table 1B. The responses of the physical-reasoning system to the Sentences > Nonwords contrast. This table reports the beta estimates, standard errors of the mean, t-values, and p-values from a linear mixed-effects model (see [Methods](#)). We first report the effects for the system as a whole, and then for each fROI group separately. For the fROI groups, we report uncorrected p-values, but we mark the values that survive the Bonferroni correction for the number of fROI groups (n=9) in **bold font**. (Two fROI groups here show a significant effect for the opposite, Nonwords > Sentences contrast.)

Task	Type	Beta	SEM	t	p
SpWM	System	1.537551	0.087604	17.551151	< 0.001
SpWM	Group MD_LH_med_sup_front	0.92688174	0.21645264	4.28214564	< 0.001
SpWM	Group MD_RH_med_sup_front	1.20964828	0.20522222	5.89433387	< 0.001
SpWM	Group MD_LH_prec_mid_front	1.5104128	0.19686781	7.6722182	< 0.001
SpWM	Group MD_RH_prec_mid_front	1.7424743	0.21176718	8.22825468	< 0.001
SpWM	Group MD_LH_insula	0.75599296	0.1167514	6.47523653	< 0.001
SpWM	Group MD_RH_insula	0.803655	0.13206182	6.08544538	< 0.001
SpWM	Group MD_LH_parietal	1.80720287	0.28656473	6.30643849	< 0.001
SpWM	Group MD_RH_parietal	2.16171833	0.32748154	6.60103869	< 0.001

Table 2A. The responses of the MD system to the Hard > Easy contrast. This table reports the beta estimates, standard errors of the mean, t-values, and p-values from a linear mixed-effects model (see [Methods](#)). We first report the effects for the system as a whole, and then for each fROI group separately. For the fROI groups, we report uncorrected p-values, but we mark the values that survive the Bonferroni correction for the number of fROI groups (n=9) in **bold font**.

Task	Type	Beta	SEM	t	p
Phys	System	0.3082425	0.05517682	5.58644875	< 0.001
Phys	Group MD_LH_med_sup_front	0.36396395	0.08676529	4.19481053	< 0.001
Phys	Group MD_RH_med_sup_front	0.22140019	0.10975274	2.0172634	0.0468
Phys	Group MD_LH_prec_mid_front	0.3170827	0.10217979	3.10318422	0.0022
Phys	Group MD_RH_prec_mid_front	0.11426385	0.11337393	1.00784943	0.3150
Phys	Group MD_LH_insula	0.07258097	0.04499141	1.61321812	0.1180
Phys	Group MD_RH_insula	-0.0406542	0.04435981	-0.9164648	0.3670
Phys	Group MD_LH_parietal	0.60637771	0.15429581	3.92996881	< 0.001
Phys	Group MD_RH_parietal	0.47255856	0.17861755	2.64564464	0.0091

Table 2B. The responses of the MD system to the Physics > Color contrast. This table reports the beta estimates, standard errors of the mean, t-values, and p-values from a linear mixed-effects model (see [Methods](#)). We first report the effects for the system as a whole, and then for each fROI group separately. For the fROI groups, we report uncorrected p-values, but we mark the values that survive the Bonferroni correction for the number of fROI groups (n=9) in **bold font**.

Task	Type	Beta	SEM	t	p
Lang	System	0.992064288	0.053534777	18.5312119	< 0.001
Lang	LH Inferior Frontal Gyrus (orbital)	1.284653795	0.152222582	8.439311569	< 0.001
Lang	LH Inferior Frontal Gyrus	1.379889923	0.155064095	8.898835843	< 0.001
Lang	LH Middle Frontal Gyrus	1.86698841	0.178961683	10.43233604	< 0.001
Lang	LH Anterior Temporal	1.389281538	0.118291459	11.74456341	< 0.001
Lang	LH Posterior Temporal	1.811737795	0.155516339	11.64982284	< 0.001

Table 3A. The responses of the language system to the Sentences > Nonwords contrast. This table reports the beta estimates, standard errors of the mean, t-values, and p-values from a linear mixed-effects model (see Methods). We first report the effects for the system as a whole, and then for each fROI separately. For the fROIs, we report uncorrected p-values, but we mark the values that survive the Bonferroni correction for the number of fROIs (n=6) in **bold font**.

Task	Type	Beta	SEM	t	p
Phys	System	0.105882318	0.038001317	2.786280264	0.0507
Phys	LH Inferior Frontal Gyrus (orbital)	0.137547462	0.058360468	2.356860173	0.0237
Phys	LH Inferior Frontal Gyrus	0.141801846	0.049455125	2.867283125	0.0067
Phys	LH Middle Frontal Gyrus	0.155651897	0.057364939	2.713362895	0.0010
Phys	LH Anterior Temporal	-0.031725077	0.034565603	-0.917822187	0.3650
Phys	LH Posterior Temporal	0.062227513	0.042287678	1.471528238	0.1490

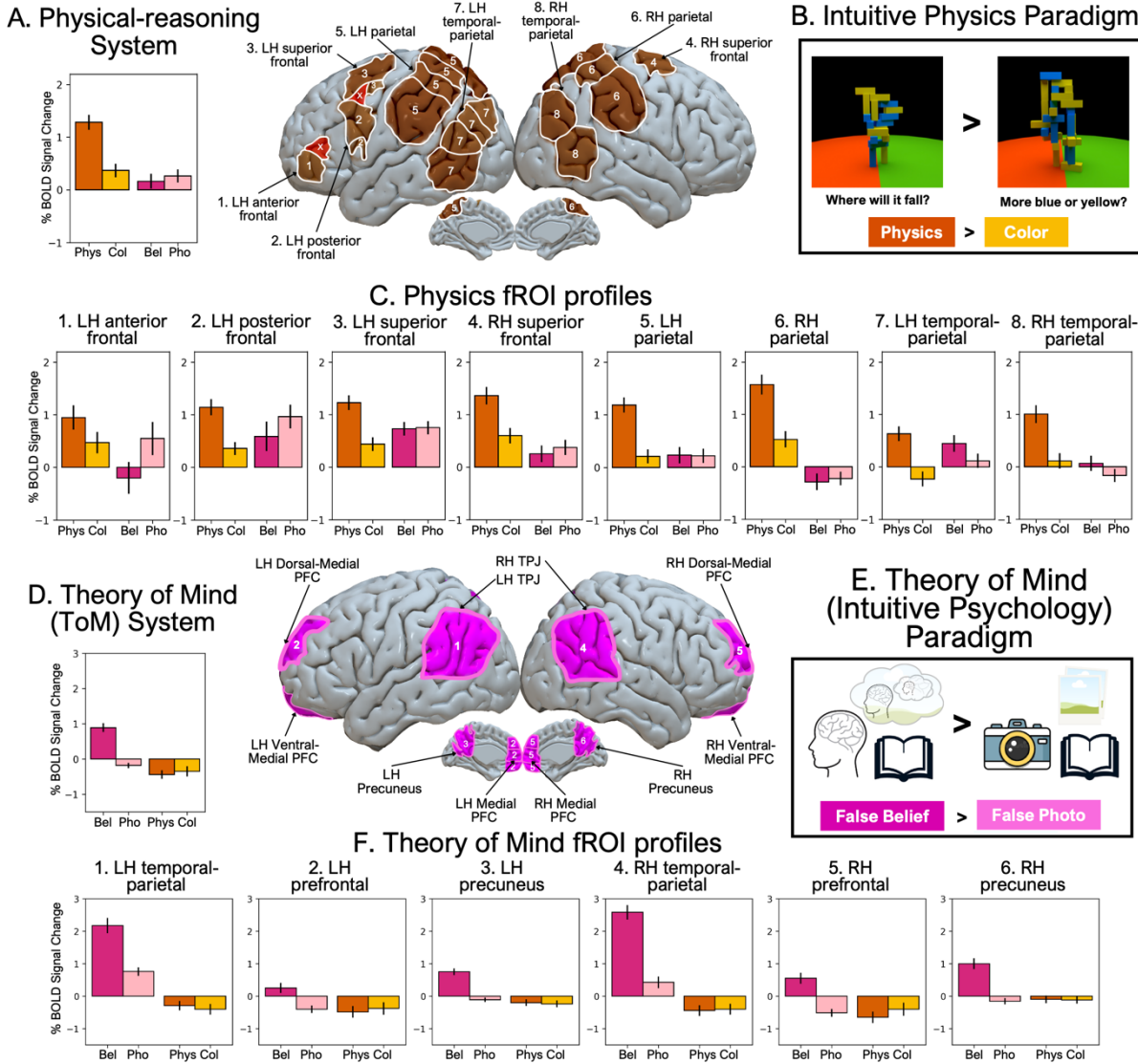
Table 3B. The responses of the language system to the Physics > Color contrast. This table reports the beta estimates, standard errors of the mean, t-values, and p-values from a linear mixed-effects model (see Methods). We first report the effects for the system as a whole, and then for each fROI separately. For the fROIs, we report uncorrected p-values, but we mark the values that survive the Bonferroni correction for the number of fROIs (n=6) in **bold font**.

	Predictor	Beta	SEM	p-value
All physical-reasoning regions	P vs. C (in ref=MD Sys)	0.31	0.05	<0.001
	P vs. C in Phys (vs. ref=MD Sys)	0.58	0.07	<0.001
Only the subset of core regions as defined by Fischer et al. (2016)	P vs. C (in ref=MD Sys)	0.31	0.05	<0.001
	P vs. C in Core (vs. ref=MD Sys)	0.70	0.08	<0.001

Table 4A. The comparison of responses to the Physics > Color contrast between the MD system and the physical-reasoning system. This table reports the estimates, standard errors of the mean, and p-values from a linear mixed-effects model (see [Methods](#)). The critical interaction between system and contrast is shown in the last row.

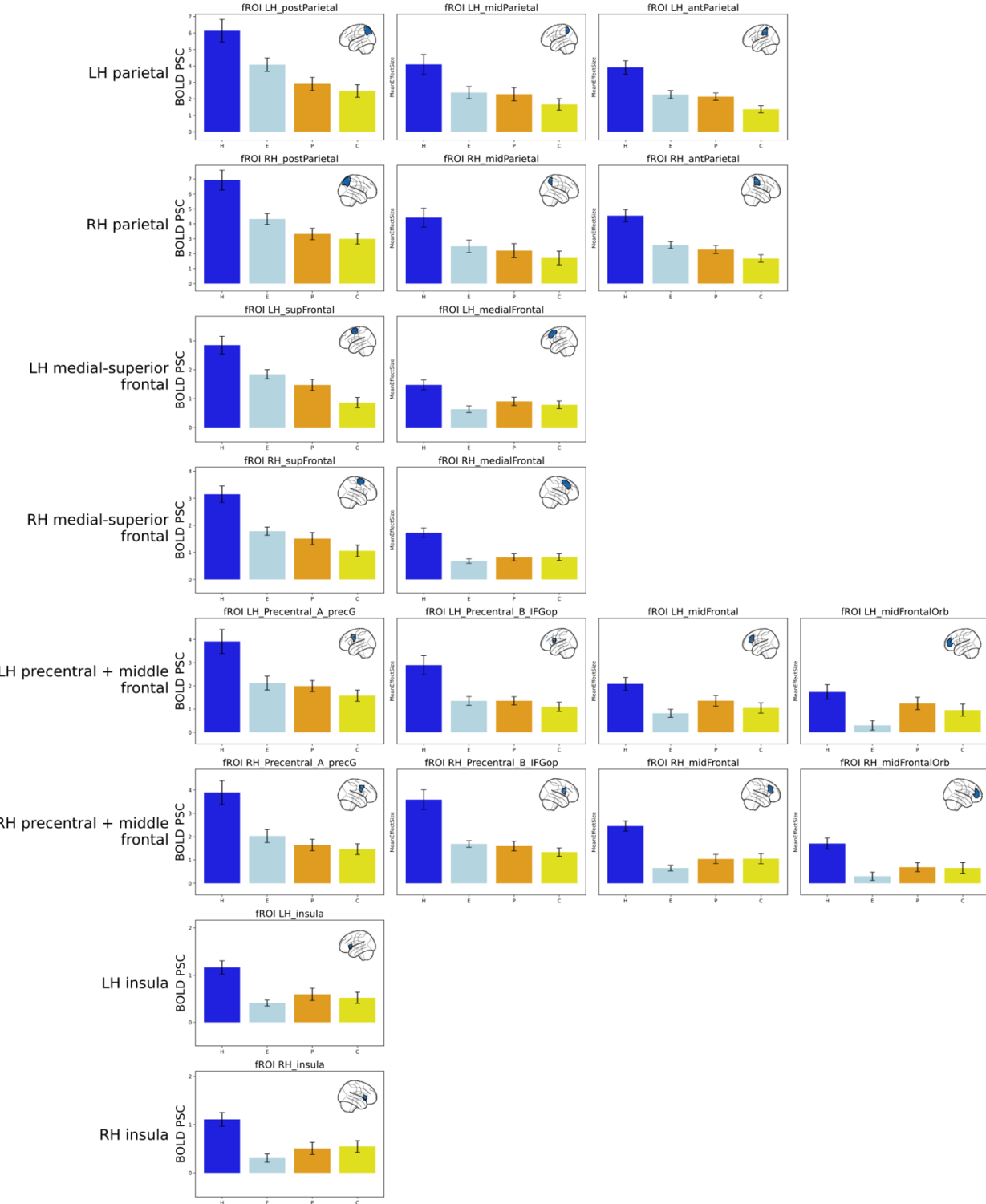
	Predictor	Beta	SEM	p-value
All physical-reasoning regions	H vs. E (in ref=MD Sys)	1.54	0.09	<0.001
	H vs. E in Phys (vs. ref=MD Sys)	-0.64	0.12	<0.001
Only the subset of core regions as defined by Fischer et al. (2016)	H vs. E (in ref=MD Sys)	1.54	0.09	<0.001
	H vs. E in Core (vs. ref=MD Sys)	-0.36	0.14	0.011

Table 4B. The comparison of responses to the Hard > Easy contrast between the MD system and the physical-reasoning system. This table reports the estimates, standard errors of the mean, and p-values from a linear mixed-effects model (see [Methods](#)). The critical interaction between system and contrast is shown in the last row.

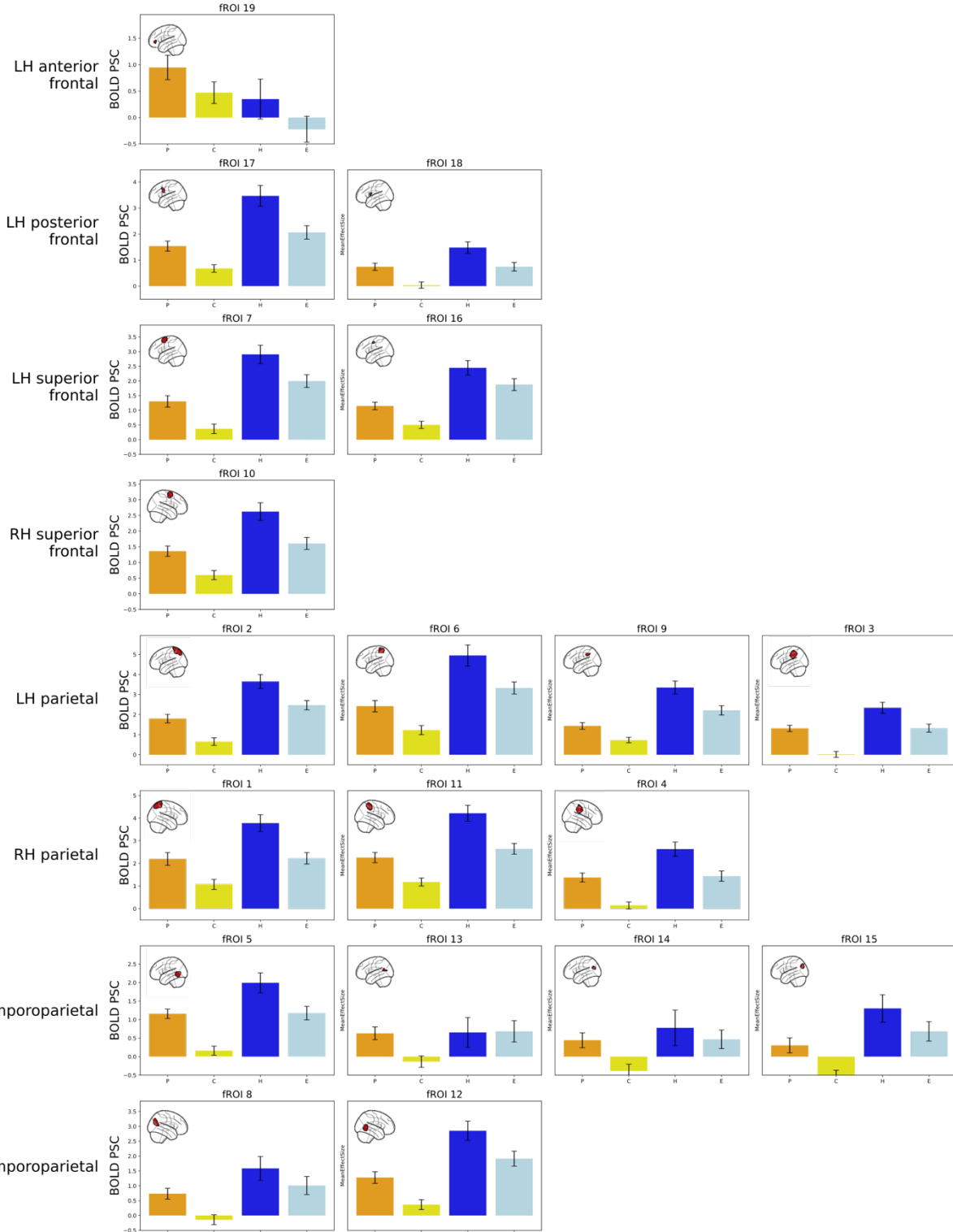


Supplementary Figure 1. The physical-reasoning system and its relationship with the Theory of Mind system. **A.** The response in the physical-reasoning fROIs to the physical-reasoning localizer and Theory of Mind (ToM) localizer conditions (Physics, Color, False Belief, False Photo), averaged across the fROIs; and the physical-reasoning parcels (excluding parcels in the probationary fROI groups 7, 8 and parcels 20, 21, shown in red; see [Methods](#)). **B.** The physical-reasoning localizer. During the critical (Physics) condition, participants answered “where will it fall?” by judging whether the block tower would fall towards the green or red side of the floor; during the control (Color) condition, participants answered “more blue or yellow?” by judging whether the block tower consisted of more yellow or blue blocks (see [Methods](#) for details). **C.** The response in the physical-reasoning fROIs, broken down by fROI group, to the physical-reasoning localizer and ToM localizer conditions (Physics, Color, False Belief, False Photo). We observe a strong Physics>Color effect in all fROI groups, probationary fROI groups (7, 8) spanning the LH and RH posterior temporal-parietal areas, outlined in red ([Table 1A](#)). **D.** The response in the ToM system fROIs to the ToM localizer and physical-reasoning localizer conditions (False Belief, False Photo, Physics, Color), averaged across the fROIs; and the ToM system parcels. **E.** The ToM localizer. Participants were tasked with reading stories and then answering short True or False reading comprehension stories at the end. During the False Belief condition, the story and comprehension question involved correctly modeling an incorrect (false) belief held by the person in the story, while

1
2
3
4 during the False Photo condition, the story and comprehension question involved correctly modeling a
5 photo, map or other type physical record with incorrect (false) information on it. F. The response in the
6 ToM system fROIs, broken down by fROI group, to the ToM localizer and physical-reasoning localizer
7 conditions (False Belief, False Photo, Physics, Color). We observe a strong False Belief>False Photo
8 effect in all fROI groups (**Supp. Table 4A**).
9
10
11
12
13
14
15
16
17
18
19
20
21
22
23
24
25
26
27
28
29
30
31
32
33
34
35
36
37
38
39
40
41
42
43
44
45
46
47
48
49
50
51
52
53
54
55
56
57
58
59
60
61
62
63
64
65



Supplementary Figure 2. The individual responses in the MD system fROIs. The response in the MD system fROIs, broken down by individual fROI, to the MD localizer and physical-reasoning localizer conditions (Hard, Easy, Physics, Color). Each of the 20 fROIs is grouped into 8 fROI groups. We observe a strong Hard>Easy effect in all individual fROIs (**Supp. Table 3A**).



Supplementary Figure 3. The individual responses in the physical-reasoning system fROIs.
The response in the physical-reasoning system fROIs, broken down by individual fROI, to the physical-reasoning localizer and MD localizer conditions (Physics, Color, Hard, Easy). Each of the 19 fROIs is grouped into 8 fROI groups. We observe a strong Physics>Color effect in all individual fROIs (**Supp. Table. 1A**).

Task	Type	Beta	SEM	t	p
Phys	System=Phys	0.88682996	0.04228111	20.9746152	< 0.001
Lang	System=Phys	-0.0757119	0.03932296	-1.9253876	0.0544
SpWM	System=Phys	0.89585529	0.07982056	11.2233654	< 0.001
ToM	System=Phys	-0.1245342	0.07203422	-1.7288196	0.0842
Phys	System=Phys (CoreRegions)	1.01288101	0.05558128	18.2234187	< 0.001
Lang	System=Phys (CoreRegions)	-0.1465097	0.03765454	-3.8908903	< 0.001
SpWM	System=Phys (CoreRegions)	1.17723892	0.10033211	11.7334215	< 0.001
ToM	System=Phys (CoreRegions)	-0.2172296	0.07060061	-3.07688	0.00224
Phys	Group Phys_LH_ant_front	0.47676937	0.12833382	3.71507201	< 0.001
Phys	Group Phys_LH_post_front	0.784105	0.10655157	7.35892502	< 0.001
Phys	Group Phys_LH_sup_front	0.78933915	0.09737534	8.10615074	< 0.001
Phys	Group Phys_RH_sup_front	0.76371005	0.09711203	7.86421699	< 0.001
Phys	Group Phys_LH_parietal	1.08557261	0.09619728	11.2848575	< 0.001
Phys	Group Phys_RH_parietal	1.14804378	0.11069309	10.3714129	< 0.001
Phys	Group Phys_LH_temp_par	0.86592093	0.0869462	9.95927305	< 0.001
Phys	Group Phys_RH_temp_par	0.89463956	0.11668926	7.66685405	< 0.001
Lang	Group Phys_LH_ant_front	-0.5601395	0.13703985	-4.0874206	< 0.001
Lang	Group Phys_LH_post_front	-0.1899408	0.11752066	-1.6162336	0.1090
Lang	Group Phys_LH_sup_front	-0.092001	0.07294022	-1.261321	0.2100
Lang	Group Phys_RH_sup_front	-0.0172135	0.04434001	-0.3882168	0.7000
Lang	Group Phys_LH_parietal	-0.2797677	0.07548286	-3.7063741	< 0.001
Lang	Group Phys_RH_parietal	-0.04827	0.06901931	-0.6993701	0.4850
Lang	Group Phys_LH_temp_par	0.13338346	0.10700407	1.24652697	0.2140
Lang	Group Phys_RH_temp_par	0.04888071	0.11172353	0.43751486	0.6630
SpWM	Group Phys_LH_ant_front	0.57151624	0.23739312	2.4074676	0.0229
SpWM	Group Phys_LH_post_front	1.07062121	0.26144144	4.09507082	< 0.001
SpWM	Group Phys_LH_sup_front	0.74060714	0.20097605	3.68505168	< 0.001
SpWM	Group Phys_RH_sup_front	1.01674138	0.13512636	7.52437498	< 0.001
SpWM	Group Phys_LH_parietal	1.23692777	0.19687521	6.28280086	< 0.001
SpWM	Group Phys_RH_parietal	1.44224084	0.18405342	7.83599038	< 0.001
SpWM	Group Phys_LH_temp_par	0.4291313	0.18567308	2.31121981	0.0218
SpWM	Group Phys_RH_temp_par	0.75711681	0.19816489	3.82064047	< 0.001
ToM	Group Phys_LH_ant_front	-0.7491802	0.19155441	-3.9110571	< 0.001
ToM	Group Phys_LH_post_front	-0.3780215	0.19529567	-1.935637	0.0575
ToM	Group Phys_LH_sup_front	-0.0219942	0.11564116	-0.1901934	0.8500
ToM	Group Phys_RH_sup_front	-0.1195793	0.09665533	-1.2371722	0.2300
ToM	Group Phys_LH_parietal	-0.3052019	0.11598385	-2.6314173	0.0094
ToM	Group Phys_RH_parietal	-0.2626403	0.13254645	-1.9814963	0.0502

ToM	Group Phys_LH_temp_par	0.33196783	0.146297	2.26913626	0.0247
ToM	Group Phys_RH_temp_par	0.23226005	0.12002291	1.93513096	0.0575

Supplementary Table 1A. The responses in the physical-reasoning system to all contrasts.

Beta estimates, standard errors of the mean, t-values, and p-values for the physical reasoning system's response to each of the four contrasts (here and elsewhere: Physics>Color (Phys), Sentences>Nonwords (Lang), Hard>Easy spatial working memory (MD), and False belief>False photo (ToM)). We report uncorrected significance values, but we mark the values that survive the Bonferroni correction for the number of fROI groups in **bold** font.

Task Comparison	Type	Beta	SEM	t	p
Lang vs. Phys	System=Phys	-1.0105566	0.08558663	-11.807412	< 0.001
SpWM vs. Phys	System=Phys	0.01521865	0.09275775	0.16406878	0.8700
ToM vs. Phys	System=Phys	-1.0164148	0.10248963	-9.9172446	< 0.001
Lang vs. Phys	System=Phys (CoreRegions)	-1.1593907	0.10678708	-10.857031	< 0.001
SpWM vs. Phys	System=Phys (CoreRegions)	0.16435791	0.11573455	1.42012836	0.0156
ToM vs. Phys	System=Phys (CoreRegions)	-1.2301106	0.12787709	-9.6194764	< 0.001
Lang vs. Phys	Phys_LH_ant_front	-1.0369089	0.3941649	-2.6306474	0.0091
SpWM vs. Phys	Phys_LH_ant_front	0.09474687	0.42719116	0.22179033	0.8250
ToM vs. Phys	Phys_LH_ant_front	-1.2259496	0.47201084	-2.5972912	0.0100
Lang vs. Phys	Phys_LH_post_front	-0.9740458	0.24917161	-3.9091366	< 0.001
SpWM vs. Phys	Phys_LH_post_front	0.28651621	0.27004918	1.0609779	0.2890
ToM vs. Phys	Phys_LH_post_front	-1.1621265	0.29838197	-3.8947612	< 0.001
Lang vs. Phys	Phys_LH_sup_front	-0.8813402	0.18563162	-4.7477913	< 0.001
SpWM vs. Phys	Phys_LH_sup_front	-0.048732	0.20118531	-0.2422245	0.8090
ToM vs. Phys	Phys_LH_sup_front	-0.8113333	0.2222931	-3.6498359	< 0.001
Lang vs. Phys	Phys_RH_sup_front	-0.7809236	0.23984519	-3.2559485	0.0013
SpWM vs. Phys	Phys_RH_sup_front	0.25303133	0.25994132	0.97341712	0.3310
ToM vs. Phys	Phys_RH_sup_front	-0.8832893	0.28721363	-3.0753741	0.0024
Lang vs. Phys	Phys_LH_parietal	-1.3653403	0.18410825	-7.4159649	< 0.001
SpWM vs. Phys	Phys_LH_parietal	0.15135515	0.1995343	0.75854204	0.4480
ToM vs. Phys	Phys_LH_parietal	-1.3907745	0.22046887	-6.3082579	< 0.001
Lang vs. Phys	Phys_RH_parietal	-1.1963138	0.20803061	-5.7506624	< 0.001
SpWM vs. Phys	Phys_RH_parietal	0.29419706	0.22546107	1.3048686	0.1920
ToM vs. Phys	Phys_RH_parietal	-1.4106841	0.2491158	-5.6627643	< 0.001
Lang vs. Phys	Phys_LH_temp_par	-0.7325375	0.17865249	-4.1003485	< 0.001
SpWM vs. Phys	Phys_LH_temp_par	-0.4367896	0.19362141	-2.2558953	0.0243
ToM vs. Phys	Phys_LH_temp_par	-0.5339531	0.21393562	-2.4958587	0.0127
Lang vs. Phys	Phys_RH_temp_par	-0.8457589	0.2328616	-3.6320237	< 0.001
SpWM vs. Phys	Phys_RH_temp_par	-0.1375228	0.25237259	-0.5449195	0.5860
ToM vs. Phys	Phys_RH_temp_par	-0.6623795	0.27885081	-2.3753903	0.0179

Supplementary Table 1B. Physical Reasoning System Response Comparison for Other Task Contrasts versus Native (Physical Reasoning) Contrast. Interaction effects for Task (the physical-reasoning task (Phys) vs. each of the other tasks) in the physical-reasoning system.

Task	Type	Beta	SEM	d	t	p
Lang	System=Lang	0.99206429	0.05353478	1.1318428	18.5312119	< 0.001
Phys	System=Lang	0.10588232	0.03800132	0.18776358	2.78628026	0.0507
SpWM	System=Lang	-0.2738053	0.06206577	-0.4188434	-4.4115343	< 0.001
ToM	System=Lang	0.54589246	0.08327175	0.49117571	6.55555418	< 0.001
Lang	LIFGorb	1.28465379	0.15222258	NA	8.43931157	< 0.001
Lang	LIFG	1.37988992	0.15506409	NA	8.89883584	< 0.001
Lang	LMFG	1.86698841	0.17896168	NA	10.432336	< 0.001
Lang	LAntTemp	1.38928154	0.11829146	NA	11.7445634	< 0.001
Lang	LPostTemp	1.81173779	0.15551634	NA	11.6498228	< 0.001
Phys	LIFGorb	0.13754746	0.05836047	NA	2.35686017	0.0237
Phys	LIFG	0.14180185	0.04945513	NA	2.86728313	0.0067
Phys	LMFG	0.1556519	0.05736494	NA	2.7133629	0.0010
Phys	LAntTemp	-0.0317251	0.0345656	NA	-0.9178222	0.3650
Phys	LPostTemp	0.06222751	0.04228768	NA	1.47152824	0.1490
SpWM	LIFGorb	-0.6764587	0.12322976	NA	-5.4894107	< 0.001
SpWM	LIFG	-0.0918744	0.08866423	NA	-1.0362062	0.3090
SpWM	LMFG	0.00697329	0.07389265	NA	0.0943705	0.9260
SpWM	LAntTemp	-0.3962753	0.06225497	NA	-6.3653591	< 0.001
SpWM	LPostTemp	-0.4429257	0.0728494	NA	-6.0800191	< 0.001
ToM	LIFGorb	0.42421005	0.11638742	NA	3.64481023	0.0016
ToM	LIFG	0.46423281	0.11930102	NA	3.89127266	< 0.001
ToM	LMFG	0.40334952	0.13864628	NA	2.90919825	0.0087
ToM	LAntTemp	0.42592481	0.07437058	NA	5.72706079	< 0.001
ToM	LPostTemp	0.61523876	0.09983752	NA	6.16240044	< 0.001

Supplementary Table 2A. The responses in the language system to all contrasts. Beta estimates, standard errors of the mean, t-values, and p-values for the language system's response to each of the four contrasts (here and elsewhere: Sentences > Nonwords (Lang), Physics > Color (Phys), Hard > Easy spatial working memory (MD), and False Belief > False Photo (ToM)). We report uncorrected significance values, but we mark the values that survive the Bonferroni correction for the number of fROI groups in **bold** font.

Task Comparison	Type	Beta	SEM	Cohen's d	t	p
Phys vs. Lang	System=Lang	-1.4534096	0.12122596	-1.0099726	-11.98926	< 0.001
SpWM vs. Lang	System=Lang	-1.8666225	0.13259863	-1.2971137	-14.077238	< 0.001
ToM vs. Lang	System=Lang	-1.0799191	0.14489274	-0.7504345	-7.4532313	< 0.001
Phys vs. Lang	LIFGorb	-1.1471063	0.29051999	-0.9464339	-3.9484592	< 0.001
SpWM vs. Lang	LIFGorb	-1.9611125	0.31777477	-1.6180395	-6.1713916	< 0.001
ToM vs. Lang	LIFGorb	-0.8604437	0.3472378	-0.7099195	-2.4779668	0.0140
Phys vs. Lang	LIFG	-1.2380881	0.25880262	-0.9412242	-4.7839086	< 0.001
SpWM vs. Lang	LIFG	-1.4717644	0.28308187	-1.1188705	-5.1990767	< 0.001
ToM vs. Lang	LIFG	-0.9156571	0.30932829	-0.6961045	-2.9601467	0.0034
Phys vs. Lang	LMFG	-1.7113365	0.28483189	-0.9878502	-6.0082335	< 0.001
SpWM vs. Lang	LMFG	-1.8600151	0.31155304	-1.0736733	-5.9701395	< 0.001
ToM vs. Lang	LMFG	-1.4636389	0.34043922	-0.8448695	-4.2992663	< 0.001
Phys vs. Lang	LAntTemp	-1.4210066	0.16362087	-1.2587258	-8.6847518	< 0.001
SpWM vs. Lang	LAntTemp	-1.7855568	0.17897076	-1.5816439	-9.9768075	< 0.001
ToM vs. Lang	LAntTemp	-0.9633567	0.19556434	-0.8533402	-4.9260347	< 0.001
Phys vs. Lang	LPostTemp	-1.7495103	0.22389131	-1.1013937	-7.8141053	< 0.001
SpWM vs. Lang	LPostTemp	-2.2546635	0.2448954	-1.4194099	-9.2066389	< 0.001
ToM vs. Lang	LPostTemp	-1.196499	0.2676013	-0.7532488	-4.4712004	< 0.001

Supplementary Table 2B. Language system response comparison for other task contrasts versus native (Language) contrast. Interaction effects for Task (the language task (Lang) vs. each of the other tasks) in the language system.

Task	Type	Beta	SEM	t	p
Lang	System=MD	-0.250448	0.03374822	-7.4210718	< 0.001
Phys	System=MD	0.3082425	0.05517682	5.58644875	< 0.001
SpWM	System=MD	1.537551	0.087604	17.551151	< 0.001
ToM	System=MD	-0.0905343	0.05894839	-1.535823	0.1250
Lang	Group MD_LH_parietal	-0.4017876	0.08422497	-4.7704097	< 0.001
Lang	Group MD_RH_parietal	-0.1968671	0.07650859	-2.5731376	0.0110
Lang	Group MD_LH_med_sup_front	-0.1545382	0.06077965	-2.5425982	0.0126
Lang	Group MD_RH_med_sup_front	-0.1421019	0.05465392	-2.6000307	0.0108
Lang	Group MD_LH_prec_mid_front	-0.3456644	0.10976758	-3.1490575	0.0019
Lang	Group MD_RH_prec_mid_front	-0.2654022	0.09379698	-2.8295389	0.0051
Lang	Group MD_LH_insula	-0.049402	0.05373297	-0.9193988	0.3650
Lang	Group MD_RH_insula	-0.1260463	0.05006346	-2.5177304	0.0170
Phys	Group MD_LH_parietal	0.60637771	0.15429581	3.92996881	< 0.001
Phys	Group MD_RH_parietal	0.47255856	0.17861755	2.64564464	0.0091
Phys	Group MD_LH_med_sup_front	0.36396395	0.08676529	4.19481053	< 0.001
Phys	Group MD_RH_med_sup_front	0.22140019	0.10975274	2.0172634	0.0468
Phys	Group MD_LH_prec_mid_front	0.3170827	0.10217979	3.10318422	0.0022
Phys	Group MD_RH_prec_mid_front	0.11426385	0.11337393	1.00784943	0.3150
Phys	Group MD_LH_insula	0.07258097	0.04499141	1.61321812	0.1180
Phys	Group MD_RH_insula	-0.0406542	0.04435981	-0.9164648	0.3670
SpWM	Group MD_LH_parietal	1.80720287	0.28656473	6.30643849	< 0.001
SpWM	Group MD_RH_parietal	2.16171833	0.32748154	6.60103869	< 0.001
SpWM	Group MD_LH_med_sup_front	0.92688174	0.21645264	4.28214564	< 0.001
SpWM	Group MD_RH_med_sup_front	1.20964828	0.20522222	5.89433387	< 0.001
SpWM	Group MD_LH_prec_mid_front	1.5104128	0.19686781	7.6722182	< 0.001
SpWM	Group MD_RH_prec_mid_front	1.7424743	0.21176718	8.22825468	< 0.001
SpWM	Group MD_LH_insula	0.75599296	0.1167514	6.47523653	< 0.001
SpWM	Group MD_RH_insula	0.803655	0.13206182	6.08544538	< 0.001
ToM	Group MD_LH_parietal	-0.2692161	0.15812686	-1.7025326	0.0929
ToM	Group MD_RH_parietal	-0.1868209	0.1624008	-1.1503694	0.2540
ToM	Group MD_LH_med_sup_front	0.07094477	0.08215237	0.86357541	0.3930
ToM	Group MD_RH_med_sup_front	0.00669647	0.0725615	0.09228677	0.9270
ToM	Group MD_LH_prec_mid_front	-0.1043939	0.17844671	-0.5850146	0.5600
ToM	Group MD_RH_prec_mid_front	-0.0521522	0.14118538	-0.3693882	0.7130
ToM	Group MD_LH_insula	0.054413	0.07734995	0.70346522	0.4930
ToM	Group MD_RH_insula	-0.0260856	0.07790523	-0.3348376	0.7430

1
 2
 3
 4 **Supplementary Table 3A. The responses in the MD system to all contrasts.** Beta estimates,
 5 standard errors of the mean, t-values, and p-values for the MD system's response to each of the
 6 four contrasts (here and elsewhere: Hard > Easy spatial working memory (MD),
 7 Sentences > Nonwords (Lang), Physics > Color (Phys), and False Belief> False Photo (ToM)).
 8 We report uncorrected significance values, but we mark the values that survive the Bonferroni
 9 correction for the number of fROI groups in **bold** font.
 10
 11
 12
 13

Task Comparison	Type	Beta	SEM	t	p
Lang vs. SpWM	System=MD	-1.787998964	0.102302771	-17.4775223	< 0.001
Phys vs. SpWM	System=MD	-1.229308499	0.105160593	-11.68982089	< 0.001
ToM vs. SpWM	System=MD	-1.628085296	0.124996117	-13.02508694	< 0.001
Lang vs. SpWM	MD_LH_parietal	-2.208990486	0.300074014	-7.361485443	< 0.001
Phys vs. SpWM	MD_LH_parietal	-1.200825157	0.308456564	-3.893012164	< 0.001
ToM vs. SpWM	MD_LH_parietal	-2.076419003	0.366638032	-5.6634032	< 0.001
Lang vs. SpWM	MD_RH_parietal	-2.358585455	0.326001276	-7.234896389	< 0.001
Phys vs. SpWM	MD_RH_parietal	-1.68915977	0.335108103	-5.040641379	< 0.001
ToM vs. SpWM	MD_RH_parietal	-2.348539244	0.398316617	-5.896161851	< 0.001
Lang vs. SpWM	MD_LH_med_sup_front	-1.081419966	0.195974238	-5.518174115	< 0.001
Phys vs. SpWM	MD_LH_med_sup_front	-0.562917791	0.201448767	-2.794347166	0.0055
ToM vs. SpWM	MD_LH_med_sup_front	-0.855936972	0.239446288	-3.574651245	< 0.001
Lang vs. SpWM	MD_RH_med_sup_front	-1.351750146	0.200417403	-6.744674488	< 0.001
Phys vs. SpWM	MD_RH_med_sup_front	-0.988248093	0.206016052	-4.796947053	< 0.001
ToM vs. SpWM	MD_RH_med_sup_front	-1.202951816	0.24487506	-4.912512587	< 0.001
Lang vs. SpWM	MD_LH_prec_mid_front	-1.856077213	0.214333788	-8.65975088	< 0.001
Phys vs. SpWM	MD_LH_prec_mid_front	-1.193330106	0.220321191	-5.416320159	< 0.001
ToM vs. SpWM	MD_LH_prec_mid_front	-1.614806738	0.261878452	-6.166245153	< 0.001
Lang vs. SpWM	MD_RH_prec_mid_front	-2.007876524	0.208925277	-9.610500721	< 0.001
Phys vs. SpWM	MD_RH_prec_mid_front	-1.628210451	0.214761592	-7.581478755	< 0.001
ToM vs. SpWM	MD_RH_prec_mid_front	-1.794626521	0.255270196	-7.030301814	< 0.001
Lang vs. SpWM	MD_LH_insula	-0.805394987	0.166317553	-4.842513457	< 0.001
Phys vs. SpWM	MD_LH_insula	-0.683411991	0.170963624	-3.997411702	< 0.001
ToM vs. SpWM	MD_LH_insula	-0.701579957	0.203210999	-3.452470387	< 0.001
Lang vs. SpWM	MD_RH_insula	-0.929701303	0.176276044	-5.274121679	< 0.001
Phys vs. SpWM	MD_RH_insula	-0.844309207	0.181200305	-4.659535247	< 0.001
ToM vs. SpWM	MD_RH_insula	-0.8297406	0.215378536	-3.852475818	< 0.001

55
 56 **Supplementary Table 3B. MD system response comparison for other task contrasts versus**
 57 **native (MD) contrast.** Interaction effects for Task (the spatial working memory task (MD) vs.
 58 each of the other tasks) in the MD system.
 59
 60
 61
 62
 63
 64
 65

Task	Type	Beta	SEM	t	p
Lang	System=ToM	-0.0466322	0.06144653	-0.7589075	0.4480
Phys	System=ToM	-0.0925176	0.06241724	-1.482245	0.1390
SpWM	System=ToM	-1.0715183	0.13682159	-7.8315	< 0.001
ToM	System=ToM	1.0755126	0.07014774	15.3321051	< 0.001
Lang	LH_TPJ	0.20165395	0.11896068	1.69513108	0.1060
Lang	LH_DMPFC	-0.105776	0.16039488	-0.6594721	0.5170
Lang	LH_MMPFC	-0.2411785	0.13115445	-1.838889	0.0808
Lang	LH_VMPFC	0.06325786	0.09035825	0.70007835	0.4920
Lang	LH_PC	-0.0622847	0.06451283	-0.9654617	0.3460
Lang	RH_TPJ	0.12524786	0.11178247	1.12046064	0.2760
Lang	RH_DMPFC	-0.0844114	0.14856681	-0.5681712	0.5760
Lang	RH_MMPFC	-0.3109508	0.13257273	-2.3455112	0.0294
Lang	RH_VMPFC	0.02768452	0.08412656	0.32908184	0.7460
Lang	RH_PC	-0.0795652	0.06269888	-1.2690057	0.2190
Phys	LH_TPJ	0.11198057	0.06991635	1.60163642	0.1250
Phys	LH_DMPFC	-0.084489	0.08226043	-1.027091	0.3170
Phys	LH_MMPFC	-0.1305201	0.12386433	-1.0537347	0.3050
Phys	LH_VMPFC	-0.099595	0.07355424	-1.3540354	0.1910
Phys	LH_PC	0.03882286	0.05543189	0.70037044	0.4920
Phys	RH_TPJ	-0.0447329	0.06221285	-0.71903	0.4800
Phys	RH_DMPFC	-0.3097736	0.10869191	-2.850015	0.0099
Phys	RH_MMPFC	-0.2698417	0.13435199	-2.0084683	0.0583
Phys	RH_VMPFC	-0.1569344	0.06260388	-2.5067843	0.0209
Phys	RH_PC	0.01990695	0.05124158	0.38849214	0.7020
SpWM	LH_TPJ	-0.9029304	0.17918943	-5.0389714	< 0.001
SpWM	LH_DMPFC	-1.4458423	0.29991551	-4.8208322	< 0.001
SpWM	LH_MMPFC	-1.4475622	0.29795169	-4.8583788	< 0.001
SpWM	LH_VMPFC	-1.1539525	0.21564126	-5.3512602	< 0.001
SpWM	LH_PC	-0.6107448	0.11598964	-5.2655114	< 0.001
SpWM	RH_TPJ	-0.8328252	0.1905336	-4.3710148	0.0011
SpWM	RH_DMPFC	-1.6242154	0.35699554	-4.5496798	< 0.001
SpWM	RH_MMPFC	-1.2830995	0.41997103	-3.0552095	0.0109
SpWM	RH_VMPFC	-1.0903293	0.15790029	-6.9051757	< 0.001
SpWM	RH_PC	-0.3236812	0.11983837	-2.700981	0.0206
ToM	LH_TPJ	1.41718843	0.1559522	9.08732577	< 0.001
ToM	LH_DMPFC	0.95689976	0.18387382	5.20411091	< 0.001
ToM	LH_MMPFC	0.47253605	0.21836789	2.16394479	0.0427

ToM	LH_VMPFC	0.52742571	0.09930946	5.31093122	< 0.001
ToM	LH_PC	0.86036043	0.0987994	8.70815461	< 0.001
ToM	RH_TPJ	2.15471948	0.20609932	10.4547629	< 0.001
ToM	RH_DMPFC	1.42201586	0.24242587	5.86577601	< 0.001
ToM	RH_MMPFC	1.07536319	0.16148225	6.65932732	< 0.001
ToM	RH_VMPFC	0.71351176	0.12361665	5.77197114	< 0.001
ToM	RH_PC	1.15510533	0.12149016	9.50780986	< 0.001

Supplementary Table 4A. The responses in the Theory of Mind system to all contrasts. Beta estimates, standard errors of the mean, t-values, and p-values for the Theory of Mind system's response to each of the four contrasts (here and elsewhere: False Belief>False Photo (ToM), Sentences > Nonwords (Lang), Physics > Color (Phys), and Hard > Easy spatial working memory (MD)). We report uncorrected significance values, but we mark the values that survive the Bonferroni correction for the number of fROI groups in **bold** font.

Task Comparison	Type	Beta	SEM	t	p
Lang vs. ToM	System=ToM	-1.122144833	0.122522277	-9.158700455	< 0.001
Phys vs. ToM	System=ToM	-1.168030238	0.122522277	-9.533207083	< 0.001
SpWM vs. ToM	System=ToM	-2.147030867	0.143670105	-14.94417278	< 0.001
Lang vs. ToM	ROI 1	-1.215534476	0.311181359	-3.906193091	< 0.001
Phys vs. ToM	ROI 1	-1.305207857	0.311181359	-4.19436389	< 0.001
SpWM vs. ToM	ROI 1	-2.320118845	0.364892488	-6.358362863	< 0.001
Lang vs. ToM	ROI 2	-1.062675714	0.38317148	-2.773368504	0.0064
Phys vs. ToM	ROI 2	-1.041388714	0.38317148	-2.717813743	0.0075
SpWM vs. ToM	ROI 2	-2.402742095	0.449308387	-5.347645769	< 0.001
Lang vs. ToM	ROI 3	-0.713714524	0.415836209	-1.716335683	0.0886
Phys vs. ToM	ROI 3	-0.60305619	0.415836209	-1.450225299	0.1500
SpWM vs. ToM	ROI 3	-1.920098214	0.487611177	-3.937764975	< 0.001
Lang vs. ToM	ROI 4	-0.464167857	0.393318471	-1.180132365	0.2400
Phys vs. ToM	ROI 4	-0.627020762	0.393318471	-1.594180819	0.1130
SpWM vs. ToM	ROI 4	-1.681378214	0.461206789	-3.645605954	< 0.001
Lang vs. ToM	ROI 5	-0.922645095	0.210467895	-4.383780688	< 0.001
Phys vs. ToM	ROI 5	-0.821537571	0.210467895	-3.903386642	< 0.001
SpWM vs. ToM	ROI 5	-1.471105179	0.246795483	-5.960826991	< 0.001
Lang vs. ToM	ROI 6	-2.029471619	0.295157367	-6.875896869	< 0.001
Phys vs. ToM	ROI 6	-2.199452381	0.295157367	-7.451795629	< 0.001
SpWM vs. ToM	ROI 6	-2.987544643	0.346102692	-8.631960143	< 0.001
Lang vs. ToM	ROI 7	-1.506427238	0.431105769	-3.494333287	< 0.001
Phys vs. ToM	ROI 7	-1.731789429	0.431105769	-4.017087114	< 0.001

1	SpWM vs. ToM	ROI 7	-3.046231274	0.505516323	-6.025980043	< 0.001
2	Lang vs. ToM	ROI 8	-1.386314	0.435265522	-3.184984633	0.0018
3	Phys vs. ToM	ROI 8	-1.345204905	0.435265522	-3.090538615	0.0025
4	SpWM vs. ToM	ROI 8	-2.35846269	0.510394066	-4.620866201	< 0.001
5	Lang vs. ToM	ROI 9	-0.685827238	0.340782608	-2.012506574	0.0464
6	Phys vs. ToM	ROI 9	-0.87044619	0.340782608	-2.5542565	0.0119
7	SpWM vs. ToM	ROI 9	-1.803841012	0.399603028	-4.514082438	< 0.001
8	Lang vs. ToM	ROI 10	-1.234670571	0.195780694	-6.306395928	< 0.001
9	Phys vs. ToM	ROI 10	-1.135198381	0.195780694	-5.798316258	< 0.001
10	SpWM vs. ToM	ROI 10	-1.4787865	0.229573213	-6.441459262	< 0.001

Supplementary Table 4B. Theory of Mind system response comparison for other task contrasts versus native (Theory of Mind) contrast. Interaction effects for Task (the Theory of Mind task (ToM) vs. each of the other tasks) in the Theory of Mind system.

1
2
3
4
5
6
7 **References**

- 8 Amalric, Marie, and Stanislas Dehaene. "A Distinct Cortical Network for Mathematical
9 Knowledge in the Human Brain." *NeuroImage* 189 (April 1, 2019): 19–31.
<https://doi.org/10.1016/j.neuroimage.2019.01.001>.
- 10 Amunts, Katrin, Marianne Lenzen, Angela D. Friederici, Axel Schleicher, Patricia Morosan,
11 Nicola Palomero-Gallagher, and Karl Zilles. "Broca's Region: Novel Organizational
12 Principles and Multiple Receptor Mapping." Edited by David Poeppel. *PLoS Biology* 8, no.
13 9 (September 21, 2010): e1000489. <https://doi.org/10.1371/journal.pbio.1000489>.
- 14 Ashburner, John, and Karl J. Friston. "Unified Segmentation." *NeuroImage* 26, no. 3 (July 1,
15 2005): 839–51. <https://doi.org/10.1016/j.neuroimage.2005.02.018>.
- 16 Assem, Moataz, Idan Asher Blank, Zachary Mineroff, Ahmet Ademoglu, and Evelina
17 Fedorenko. "Activity in the Fronto-Parietal Multiple-Demand Network Is Robustly
18 Associated with Individual Differences in Working Memory and Fluid Intelligence."
19 *Cortex; a Journal Devoted to the Study of the Nervous System and Behavior* 131 (July 15,
20 2020): 1. <https://doi.org/10.1016/j.cortex.2020.06.013>.
- 21 Assem, Moataz, Matthew F Glasser, David C Van Essen, and John Duncan. "A Domain-General
22 Cognitive Core Defined in Multimodally Parcellated Human Cortex." *Cerebral Cortex* 30,
23 no. 8 (June 30, 2020): 4361–80. <https://doi.org/10.1093/cercor/bhaa023>.
- 24 Basilakos, Alexandra, Kimberly G Smith, Paul Fillmore, Julius Fridriksson, and Evelina
25 Fedorenko. "Functional Characterization of the Human Speech Articulation Network."
26 *Cerebral Cortex* 28, no. 5 (May 1, 2018): 1816–30. <https://doi.org/10.1093/cercor/bhx100>.
- 27 Bates, Douglas, Martin Mächler, Ben Bolker, and Steve Walker. "Fitting Linear Mixed-Effects
28 Models Using Lme4." *Journal of Statistical Software* 67, no. 1 (2015).
<https://doi.org/10.18637/jss.v067.i01>.
- 29 Battaglia, Peter W., Jessica B. Hamrick, and Joshua B. Tenenbaum. "Simulation as an Engine of
30 Physical Scene Understanding." *Proceedings of the National Academy of Sciences* 110, no.
31 45 (November 5, 2013): 18327–32. <https://doi.org/10.1073/pnas.1306572110>.
- 32 Benjamini, Yoav, and Daniel Yekutieli. "The Control of the False Discovery Rate in Multiple
33 Testing under Dependency." *The Annals of Statistics* 29, no. 4 (August 2001): 1165–88.
<https://doi.org/10.1214/aos/1013699998>.
- 34 Blank, Idan, Zuzanna Balewski, Kyle Mahowald, and Evelina Fedorenko. "Syntactic Processing
35 Is Distributed across the Language System." *NeuroImage* 127 (February 15, 2016): 307–23.
<https://doi.org/10.1016/j.neuroimage.2015.11.069>.
- 36 Blank, Idan, Nancy Kanwisher, and Evelina Fedorenko. "A Functional Dissociation between
37 Language and Multiple-Demand Systems Revealed in Patterns of BOLD Signal
38 Fluctuations." *Journal of Neurophysiology* 112, no. 5 (September 1, 2014): 1105–18.
<https://doi.org/10.1152/jn.00884.2013>.
- 39 Bozic, Mirjana, Elisabeth Fonteneau, Li Su, and William D. Marslen-Wilson. "Grammatical
40 Analysis as a Distributed Neurobiological Function." *Human Brain Mapping* 36, no. 3
41 (November 24, 2014): 1190. <https://doi.org/10.1002/hbm.22696>.
- 42 Braga, Rodrigo M., Lauren M. DiNicola, Hannah C. Becker, and Randy L. Buckner. "Situating
43 the Left-Lateralized Language Network in the Broader Organization of Multiple Specialized
44 Large-Scale Distributed Networks." *Journal of Neurophysiology* 124, no. 5 (November
45 2020): 1415–48. <https://doi.org/10.1152/jn.00753.2019>.

- 1
2
3
4 Broca, M Paul. "Remarques sur le siège de la faculté du langage articulé, suivies d'une
5 observation d'aphémie (perte de la parole)." *Bulletin et mémoires de la Société Anatomique*
6 *de Paris* 6 (1861): 330–57.
7
8 Chen, Xuanyi, Josef Affourtit, Rachel Ryskin, Tamar I Regev, Samuel Norman-Haignere,
9 Olessia Jouravlev, Saima Malik-Moraleda, Hope Kean, Rosemary Varley, and Evelina
10 Fedorenko. "The Human Language System, Including Its Inferior Frontal Component in
11 'Broca's Area,' Does Not Support Music Perception." *Cerebral Cortex* 33, no. 12 (June 8,
12 2023): 7904–29. <https://doi.org/10.1093/cercor/bhad087>.
13
14 Coetzee, John P., and Martin M. Monti. "At the Core of Reasoning: Dissociating Deductive and
15 Non-deductive Load." *Human Brain Mapping* 39, no. 4 (2018): 1850–61.
16 <https://doi.org/10.1002/hbm.23979>.
17
18 Cohen, J. D., T. S. Braver, and R. C. O'Reilly. "A Computational Approach to Prefrontal Cortex,
19 Cognitive Control and Schizophrenia: Recent Developments and Current Challenges."
20 *Philosophical Transactions of the Royal Society of London. Series B, Biological Sciences*
21 351, no. 1346 (October 29, 1996): 1515–27. <https://doi.org/10.1098/rstb.1996.0138>.
22
23 Cole, Michael W., and Walter Schneider. "The Cognitive Control Network: Integrated Cortical
24 Regions with Dissociable Functions." *NeuroImage* 37, no. 1 (August 1, 2007): 343–60.
25 <https://doi.org/10.1016/j.neuroimage.2007.03.071>.
26
27 Diacheck, Evgeniia, Idan Blank, Matthew Siegelman, Josef Affourtit, and Evelina Fedorenko.
28 "The Domain-General Multiple Demand (MD) Network Does Not Support Core Aspects of
29 Language Comprehension: A Large-Scale fMRI Investigation." *Journal of Neuroscience*,
30 April 21, 2020. <https://doi.org/10.1523/JNEUROSCI.2036-19.2020>.
31
32 DiNicola, Lauren M., Wendy Sun, and Randy L. Buckner. "Side-by-Side Regions in
33 Dorsolateral Prefrontal Cortex Estimated within the Individual Respond Differentially to
34 Domain-Specific and Domain-Flexible Processes." *Journal of Neurophysiology* 130, no. 6
35 (December 2023): 1602–15. <https://doi.org/10.1152/jn.00277.2023>.
36
37 Dodell-Feder, David, Jorie Koster-Hale, Marina Bedny, and Rebecca Saxe. "fMRI Item Analysis
38 in a Theory of Mind Task." *NeuroImage* 55, no. 2 (March 15, 2011): 705–12.
39 <https://doi.org/10.1016/j.neuroimage.2010.12.040>.
40
41 Dosenbach, Nico U. F., Kristina M. Visscher, Erica D. Palmer, Francis M. Miezin, Kristin K.
42 Wenger, Hyunseon C. Kang, E. Darcy Burgund, Ansley L. Grimes, Bradley L. Schlaggar,
43 and Steven E. Petersen. "A Core System for the Implementation of Task Sets." *Neuron* 50,
44 no. 5 (June 1, 2006): 799–812. <https://doi.org/10.1016/j.neuron.2006.04.031>.
45
46 Du, Jingnan, Lauren M. DiNicola, Peter A. Angeli, Noam Saadon-Grosman, Wendy Sun,
47 Stephanie Kaiser, Joanna Ladopoulou, et al. "Organization of the Human Cerebral Cortex
48 Estimated within Individuals: Networks, Global Topography, and Function." *Journal of*
49 *Neurophysiology* 131, no. 6 (June 1, 2024): 1014–82.
50 <https://doi.org/10.1152/jn.00308.2023>.
51
52 Duncan, John. "The Multiple-Demand (MD) System of the Primate Brain: Mental Programs for
53 Intelligent Behaviour." *Trends in Cognitive Sciences* 14, no. 4 (April 2010): 172–79.
54 <https://doi.org/10.1016/j.tics.2010.01.004>.
55
56 Duncan, John, Moataz Assem, and Sneha Shashidhara. "Integrated Intelligence from Distributed
57 Brain Activity." *Trends in Cognitive Sciences* 24, no. 10 (October 2020): 838–52.
58 <https://doi.org/10.1016/j.tics.2020.06.012>.

- Duncan, J., H. Emslie, P. Williams, R. Johnson, and C. Freer. "Intelligence and the Frontal Lobe: The Organization of Goal-Directed Behavior." *Cognitive Psychology* 30, no. 3 (June 1996): 257–303. <https://doi.org/10.1006/cogp.1996.0008>.
- Duncan, John, and Adrian M Owen. "Common Regions of the Human Frontal Lobe Recruited by Diverse Cognitive Demands." *Trends in Neurosciences* 23, no. 10 (October 2000): 475–83. [https://doi.org/10.1016/S0166-2236\(00\)01633-7](https://doi.org/10.1016/S0166-2236(00)01633-7).
- Eberly, David H. *Game Physics*. 2nd ed. Saint Louis: Chapman and Hall/CRC, 2010.
- Epstein, Russell, Edgar A. DeYoe, Daniel Z. Press, Allyson C. Rosen, and Nancy Kanwisher. "Neuropsychological Evidence for a Topographical Learning Mechanism in Parahippocampal Cortex." *Cognitive Neuropsychology* 18, no. 6 (September 2001): 481–508. <https://doi.org/10.1080/02643290125929>.
- Fedorenko, Evelina, Michael K. Behr, and Nancy Kanwisher. "Functional Specificity for High-Level Linguistic Processing in the Human Brain." *Proceedings of the National Academy of Sciences* 108, no. 39 (September 27, 2011): 16428–33. <https://doi.org/10.1073/pnas.1112937108>.
- Fedorenko, Evelina, and Idan A. Blank. "Broca's Area Is Not a Natural Kind." *Trends in Cognitive Sciences* 24, no. 4 (April 2020): 270–84. <https://doi.org/10.1016/j.tics.2020.01.001>.
- Fedorenko, Evelina, Idan Asher Blank, Matthew Siegelman, and Zachary Mineroff. "Lack of Selectivity for Syntax Relative to Word Meanings throughout the Language Network." *Cognition* 203 (October 1, 2020): 104348. <https://doi.org/10.1016/j.cognition.2020.104348>.
- Fedorenko, Evelina, Idan Blank, Matthew Siegelman, and Zachary Mineroff. "Lack of Selectivity for Syntax Relative to Word Meanings throughout the Language Network." *Cognition* 203 (June 20, 2020): 104348. <https://doi.org/10.1016/j.cognition.2020.104348>.
- Fedorenko, Evelina, John Duncan, and Nancy Kanwisher. "Broad Domain Generality in Focal Regions of Frontal and Parietal Cortex." *Proceedings of the National Academy of Sciences* 110, no. 41 (October 8, 2013): 16616–21. <https://doi.org/10.1073/pnas.1315235110>.
- . "Language-Selective and Domain-General Regions Lie Side by Side within Broca's Area." *Current Biology* 22, no. 21 (November 2012): 2059–62. <https://doi.org/10.1016/j.cub.2012.09.011>.
- Fedorenko, Evelina, Po-Jang Hsieh, Alfonso Nieto-Castañón, Susan Whitfield-Gabrieli, and Nancy Kanwisher. "New Method for fMRI Investigations of Language: Defining ROIs Functionally in Individual Subjects." *Journal of Neurophysiology* 104, no. 2 (August 2010): 1177–94. <https://doi.org/10.1152/jn.00032.2010>.
- Fedorenko, Evelina, Anna A. Ivanova, and Tamar I. Regev. "The Language Network as a Natural Kind within the Broader Landscape of the Human Brain." *Nature Reviews Neuroscience* 25, no. 5 (May 2024): 289–312. <https://doi.org/10.1038/s41583-024-00802-4>.
- Fedorenko, Evelina, Steven T. Piantadosi, and Edward A. F. Gibson. "Language Is Primarily a Tool for Communication Rather than Thought." *Nature* 630, no. 8017 (June 20, 2024): 575–86. <https://doi.org/10.1038/s41586-024-07522-w>.
- Fedorenko, Evelina, Terri L. Scott, Peter Brunner, William G. Coon, Brianna Pritchett, Gerwin Schalk, and Nancy Kanwisher. "Neural Correlate of the Construction of Sentence Meaning." *Proceedings of the National Academy of Sciences* 113, no. 41 (October 11, 2016): E6256–62. <https://doi.org/10.1073/pnas.1612132113>.
- Fedorenko, Evelina, and Rosemary Varley. "Language and Thought Are Not the Same Thing: Evidence from Neuroimaging and Neurological Patients: Language versus Thought."

1
2
3
4 *Annals of the New York Academy of Sciences* 1369, no. 1 (April 2016): 132–53.
5 <https://doi.org/10.1111/nyas.13046>.

6
7 Fischer, Jason, and Bradford Z. Mahon. “What Tool Representation, Intuitive Physics, and
8 Action Have in Common: The Brain’s First-Person Physics Engine.” *Cognitive*
9 *Neuropsychology* 38, no. 7–8 (November 17, 2021): 455–67.
10 <https://doi.org/10.1080/02643294.2022.2106126>.

11
12 Fischer, Jason, John G. Mikhael, Joshua B. Tenenbaum, and Nancy Kanwisher. “Functional
13 Neuroanatomy of Intuitive Physical Inference.” *Proceedings of the National Academy of*
14 *Sciences* 113, no. 34 (August 23, 2016). <https://doi.org/10.1073/pnas.1610344113>.

15 Flinker, Adeen, Anna Korzeniewska, Avgusta Y. Shestyuk, Piotr J. Franaszczuk, Nina F.
16 Dronkers, Robert T. Knight, and Nathan E. Crone. “Redefining the Role of Broca’s Area in
17 Speech.” *Proceedings of the National Academy of Sciences* 112, no. 9 (March 3, 2015):
18 2871–75. <https://doi.org/10.1073/pnas.1414491112>.

19
20 Fox, Michael D., Abraham Z. Snyder, Justin L. Vincent, Maurizio Corbetta, David C. Van
21 Essen, and Marcus E. Raichle. “The Human Brain Is Intrinsically Organized into Dynamic,
22 Anticorrelated Functional Networks.” *Proceedings of the National Academy of Sciences*
23 102, no. 27 (July 5, 2005): 9673–78. <https://doi.org/10.1073/pnas.0504136102>.

24
25 Friston, K. J., A. P. Holmes, J. B. Poline, P. J. Grasby, S. C. Williams, R. S. Frackowiak, and R.
26 Turner. “Analysis of fMRI Time-Series Revisited.” *NeuroImage* 2, no. 1 (March 1995): 45–
27 53. <https://doi.org/10.1006/nimg.1995.1007>.

28
29 Gleitman, Lila. “The Structural Sources of Verb Meanings.” *Language Acquisition: A Journal of*
30 *Developmental Linguistics* 1, no. 1 (1990): 3–55.
31 https://doi.org/10.1207/s15327817la0101_2.

32 Grønn, Atle, and Arnim Von Stechow. “Tense.” In *The Cambridge Handbook of Formal*
33 *Semantics*, edited by Maria Aloni and Paul Dekker, 1st ed., 313–41. Cambridge University
34 Press, 2016. <https://doi.org/10.1017/CBO9781139236157.012>.

35
36 Gurnee, Wes, and Max Tegmark. “Language Models Represent Space and Time.” arXiv, March
37 4, 2024. <https://doi.org/10.48550/arXiv.2310.02207>.

38
39 Hampshire, Adam, Roger R. Highfield, Beth L. Parkin, and Adrian M. Owen. “Fractionating
40 Human Intelligence.” *Neuron* 76, no. 6 (December 2012): 1225–37.
41 <https://doi.org/10.1016/j.neuron.2012.06.022>.

42
43 Hearne, Luke J., Luca Cocchi, Andrew Zalesky, and Jason B. Mattingley. “Reconfiguration of
44 Brain Network Architectures between Resting-State and Complexity-Dependent Cognitive
45 Reasoning.” *Journal of Neuroscience* 37, no. 35 (August 30, 2017): 8399–8411.
46 <https://doi.org/10.1523/JNEUROSCI.0485-17.2017>.

47
48 Hillis, Argye E., Melissa Work, Peter B. Barker, Michael A. Jacobs, Elisabeth L. Breese, and
49 Kristin Maurer. “Re-Examining the Brain Regions Crucial for Orchestrating Speech
50 Articulation.” *Brain: A Journal of Neurology* 127, no. Pt 7 (July 2004): 1479–87.
51 <https://doi.org/10.1093/brain/awh172>.

52 Hu, Jennifer, Hannah Small, Hope Kean, Atsushi Takahashi, Leo Zekelman, Daniel Kleinman,
53 Elizabeth Ryan, Alfonso Nieto-Castañón, Victor Ferreira, and Evelina Fedorenko.
54 “Precision fMRI Reveals That the Language-Selective Network Supports Both Phrase-
55 Structure Building and Lexical Access during Language Production.” *Cerebral Cortex* 33,
56 no. 8 (April 4, 2023): 4384–4404. <https://doi.org/10.1093/cercor/bhac350>.

1
2
3
4 Hugdahl, Kenneth, Marcus E. Raichle, Anish Mitra, and Karsten Specht. "On the Existence of a
5 Generalized Non-Specific Task-Dependent Network." *Frontiers in Human Neuroscience* 9
6 (August 6, 2015). <https://doi.org/10.3389/fnhum.2015.00430>.

7
8 Ivanova, Anna A, Shashank Srikant, Yotaro Sueoka, Hope H Kean, Riva Dhamala, Una-May
9 O'Reilly, Marina U Bers, and Evelina Fedorenko. "Comprehension of Computer Code
10 Relies Primarily on Domain-General Executive Brain Regions." *eLife* 9 (December 15,
11 2020): e58906. <https://doi.org/10.7554/eLife.58906>.

12 Julian, J. B., Evelina Fedorenko, Jason Webster, and Nancy Kanwisher. "An Algorithmic
13 Method for Functionally Defining Regions of Interest in the Ventral Visual Pathway."
14 *NeuroImage* 60, no. 4 (May 1, 2012): 2357–64.
15 <https://doi.org/10.1016/j.neuroimage.2012.02.055>.

16
17 Kanwisher, Nancy. "Functional Specificity in the Human Brain: A Window into the Functional
18 Architecture of the Mind." *Proceedings of the National Academy of Sciences* 107, no. 25
19 (June 22, 2010): 11163–70. <https://doi.org/10.1073/pnas.1005062107>.

20
21 Kanwisher, Nancy, Josh McDermott, and Marvin M. Chun. "The Fusiform Face Area: A Module
22 in Human Extrastriate Cortex Specialized for Face Perception." *The Journal of
23 Neuroscience* 17, no. 11 (June 1, 1997): 4302–11. <https://doi.org/10.1523/JNEUROSCI.17-11-04302.1997>.

24
25 Kean, Hope, Alex Fung, Josh Rule, Josh Tenenbaum, Steve Piantadosi, and Evelina Fedorenko.
26 "Deduction and Induction Dissociate in the Human Brain." *Computational Cognitive
27 Neuroscience CCN*, 2024.

28 Kleiman, Evan M., Brianna J. Turner, Szymon Fedor, Eleanor E. Beale, Jeff C. Huffman, and
29 Matthew K. Nock. "Examination of Real-Time Fluctuations in Suicidal Ideation and Its
30 Risk Factors: Results from Two Ecological Momentary Assessment Studies." *Journal of
31 Abnormal Psychology* 126, no. 6 (August 2017): 726–38.
32 <https://doi.org/10.1037/abn0000273>.

33
34 Kowalski, Robert, and Marek Sergot. "A Logic-Based Calculus of Events." *New Generation
35 Computing* 4, no. 1 (March 1, 1986): 67–95. <https://doi.org/10.1007/BF03037383>.

36 Kriegeskorte, Nikolaus. "Pattern-Information Analysis: From Stimulus Decoding to
37 Computational-Model Testing." *NeuroImage*, Multivariate Decoding and Brain Reading,
38 56, no. 2 (May 15, 2011): 411–21. <https://doi.org/10.1016/j.neuroimage.2011.01.061>.

39 Kuznetsova, Alexandra, Per B. Brockhoff, and Rune H. B. Christensen. "lmerTest Package:
40 Tests in Linear Mixed Effects Models." *Journal of Statistical Software* 82, no. 13 (2017).
41 <https://doi.org/10.18637/jss.v082.i13>.

42 Li, Lei, Jingjing Xu, Qingxiu Dong, Ce Zheng, Qi Liu, Lingpeng Kong, and Xu Sun. "Can
43 Language Models Understand Physical Concepts?" arXiv, May 23, 2023.
44 <https://doi.org/10.48550/arXiv.2305.14057>.

45 Lipkin, Benjamin, Greta Tuckute, Josef Affourtit, Hannah Small, Zachary Mineroff, Hope Kean,
46 Olessia Jouravlev, et al. "Probabilistic Atlas for the Language Network Based on Precision
47 fMRI Data from >800 Individuals." *Scientific Data* 9, no. 1 (August 29, 2022): 529.
48 <https://doi.org/10.1038/s41597-022-01645-3>.

49 Liu, Yun-Fei, Judy Kim, Colin Wilson, and Marina Bedny. "Computer Code Comprehension
50 Shares Neural Resources with Formal Logical Inference in the Fronto-Parietal Network."
51 *eLife* 9 (December 15, 2020): e59340. <https://doi.org/10.7554/eLife.59340>.

52 Long, Michael A., Kalman A. Katlowitz, Mario A. Svirsky, Rachel C. Clary, Tara McAllister
53 Byun, Najib Majaj, Hiroyuki Oya, I. I. I. Matthew A Howard, and Jeremy DW Greenlee.

- 1
2
3
4 “Functional Segregation of Cortical Regions Underlying Speech Timing and Articulation.”
5 *Neuron* 89, no. 6 (February 25, 2016): 1187. <https://doi.org/10.1016/j.neuron.2016.01.032>.
- 6 Malik-Moraleda, Saima, Dima Ayyash, Jeanne Gallée, Josef Affourtit, Malte Hoffmann, Zachary
7 Mineroff, Olessia Jouravlev, and Evelina Fedorenko. “An Investigation across 45
8 Languages and 12 Language Families Reveals a Universal Language Network.” *Nature*
9 *Neuroscience* 25, no. 8 (August 2022): 1014–19. <https://doi.org/10.1038/s41593-022-01114-5>.
- 10 Mansouri, Farshad A., Mark J Buckley, Daniel J Fehring, and Keiji Tanaka. “The Role of Primate
11 Prefrontal Cortex in Bias and Shift Between Visual Dimensions.” *Cerebral Cortex* 30, no. 1
12 (January 10, 2020): 85–99. <https://doi.org/10.1093/cercor/bhz072>.
- 13 Mansouri, Farshad A., Mark J. Buckley, Majid Mahboubi, and Keiji Tanaka. “Behavioral
14 Consequences of Selective Damage to Frontal Pole and Posterior Cingulate Cortices.”
15 *Proceedings of the National Academy of Sciences* 112, no. 29 (July 21, 2015): E3940–49.
16 <https://doi.org/10.1073/pnas.1422629112>.
- 17 Mansouri, Farshad A., Kenji Matsumoto, and Keiji Tanaka. “Prefrontal Cell Activities Related to
18 Monkeys’ Success and Failure in Adapting to Rule Changes in a Wisconsin Card Sorting
19 Test Analog.” *The Journal of Neuroscience* 26, no. 10 (March 8, 2006): 2745–56.
20 <https://doi.org/10.1523/JNEUROSCI.5238-05.2006>.
- 21 Mansouri, Farshad Alizadeh, Mark J. Buckley, and Keiji Tanaka. “The Neural Substrate and
22 Underlying Mechanisms of Executive Control Fluctuations in Primates.” *Progress in*
23 *Neurobiology* 209 (February 1, 2022): 102216.
24 <https://doi.org/10.1016/j.pneurobio.2022.102216>.
- 25 Mansouri, Farshad Alizadeh, Etienne Koechlin, Marcello G. P. Rosa, and Mark J. Buckley.
26 “Managing Competing Goals - a Key Role for the Frontopolar Cortex.” *Nature Reviews.*
27 *Neuroscience* 18, no. 11 (November 2017): 645–57. <https://doi.org/10.1038/nrn.2017.111>.
- 28 Marks, Samuel, and Max Tegmark. “The Geometry of Truth: Emergent Linear Structure in
29 Large Language Model Representations of True/False Datasets.” arXiv, August 19, 2024.
30 <https://doi.org/10.48550/arXiv.2310.06824>.
- 31 McCarthy, J., and P. J. Hayes. “Some Philosophical Problems From the Standpoint of Artificial
32 Intelligence.” *Machine Intelligence* 4 (1969): 463–502.
- 33 Miller, E. K., and J. D. Cohen. “An Integrative Theory of Prefrontal Cortex Function.” *Annual*
34 *Review of Neuroscience* 24 (2001): 167–202.
35 <https://doi.org/10.1146/annurev.neuro.24.1.167>.
- 36 Mitko, Alex, Ana Navarro-Cebrián, Sarah Cormiea, and Jason Fischer. “A Dedicated Mental
37 Resource for Intuitive Physics.” *iScience* 27, no. 1 (January 19, 2024): 108607.
38 <https://doi.org/10.1016/j.isci.2023.108607>.
- 39 Moens, Marc. “Tense, Aspect and Temporal Reference.,” 1987.
40 <https://era.ed.ac.uk/handle/1842/5369>.
- 41 Moens, Marc, and Mark Steedman. “Temporal Ontology and Temporal Reference.”
42 *Computational Linguistics* 14, no. 2 (1988): 15–28.
- 43 Monti, Martin M., Lawrence M. Parsons, and Daniel N. Osherson. “Thought Beyond Language:
44 Neural Dissociation of Algebra and Natural Language.” *Psychological Science* 23, no. 8
45 (August 2012): 914–22. <https://doi.org/10.1177/0956797612437427>.
- 46 Nanda, Neel, Andrew Lee, and Martin Wattenberg. “Emergent Linear Representations in World
47 Models of Self-Supervised Sequence Models.” arXiv, September 7, 2023.
48 <https://doi.org/10.48550/arXiv.2309.00941>.

- Niendam, Tara A., Angela R. Laird, Kimberly L. Ray, Y. Monica Dean, David C. Glahn, and Cameron S. Carter. "Meta-Analytic Evidence for a Superordinate Cognitive Control Network Subserving Diverse Executive Functions." *Cognitive, Affective, & Behavioral Neuroscience* 12, no. 2 (June 1, 2012): 241–68. <https://doi.org/10.3758/s13415-011-0083-5>.
- Nieto-Castañon, Alfonso. *Handbook of Functional Connectivity Magnetic Resonance Imaging Methods in CONN*. Hilbert Press, 2020. <https://doi.org/10.56441/hilbertpress.2207.6598>.
- Nieto-Castañon, Alfonso, and Evelina Fedorenko. "Subject-Specific Functional Localizers Increase Sensitivity and Functional Resolution of Multi-Subject Analyses." *NeuroImage* 63, no. 3 (November 2012): 1646–69. <https://doi.org/10.1016/j.neuroimage.2012.06.065>.
- Partee, Barbara H. "Nominal and Temporal Anaphora." *Linguistics and Philosophy* 7, no. 3 (1984): 243–86. <https://doi.org/10.1007/bf00627707>.
- Partee, Barbara Hall. "Some Structural Analogies Between Tenses and Pronouns in English." *Journal of Philosophy* 70, no. 18 (1973): 601–9. <https://doi.org/10.2307/2025024>.
- Pinto, Javier, and Raymond Reiter. "Temporal Reasoning in Logic Programming: A Case for the Situation Calculus," June 24, 1993. <https://doi.org/10.7551/mitpress/4305.003.0023>.
- Pramod, Rt, Michael A Cohen, Joshua B Tenenbaum, and Nancy Kanwisher. "Invariant Representation of Physical Stability in the Human Brain." *eLife* 11 (May 30, 2022): e71736. <https://doi.org/10.7554/eLife.71736>.
- Pramod, R.T., Hutchison, S. & Kanwisher N. (in preparation). Intuitive Physical Reasoning and Multiple Demand Systems Comprise Dissociable Cortical Networks.
- Pramod, R. T., Jessica Chomik, Laura Schulz, and Nancy Kanwisher. "A Region in Human Left Prefrontal Cortex Selectively Engaged in Causal Reasoning." *Proceedings of the Annual Meeting of the Cognitive Science Society* 46, no. 0 (2024). <https://escholarship.org/uc/item/6ms537c4>.
- Pulman, Stephen G. "Aspectual Shift as Type Coercion." *Transactions of the Philological Society* 95, no. 2 (November 1997): 279–317. <https://doi.org/10.1111/1467-968X.00020>.
- Regev, Tamar I., Colton Casto, Eghbal A. Hosseini, Markus Adamek, Anthony L. Ritaccio, Jon T. Willie, Peter Brunner, and Evelina Fedorenko. "Neural Populations in the Language Network Differ in the Size of Their Temporal Receptive Windows." *Nature Human Behaviour*, August 26, 2024. <https://doi.org/10.1038/s41562-024-01944-2>.
- Saxe, R., and N. Kanwisher. "People Thinking about Thinking People. The Role of the Temporo-Parietal Junction in 'Theory of Mind.'" *NeuroImage* 19, no. 4 (August 2003): 1835–42. [https://doi.org/10.1016/s1053-8119\(03\)00230-1](https://doi.org/10.1016/s1053-8119(03)00230-1).
- Saxe, Rebecca, and Lindsey J. Powell. "It's the Thought That Counts: Specific Brain Regions for One Component of Theory of Mind." *Psychological Science* 17, no. 8 (August 2006): 692–99. <https://doi.org/10.1111/j.1467-9280.2006.01768.x>.
- Schwettmann, Sarah, Joshua B Tenenbaum, and Nancy Kanwisher. "Invariant Representations of Mass in the Human Brain." *eLife* 8 (December 17, 2019): e46619. <https://doi.org/10.7554/eLife.46619>.
- Scott, Terri L., Jeanne Gallée, and Evelina Fedorenko. "A New Fun and Robust Version of an fMRI Localizer for the Frontotemporal Language System." *Cognitive Neuroscience* 8, no. 3 (July 3, 2017): 167–76. <https://doi.org/10.1080/17588928.2016.1201466>.
- Shain, Cory, Idan A. Blank, Evelina Fedorenko, Edward Gibson, and William Schuler. "Robust Effects of Working Memory Demand during Naturalistic Language Comprehension in Language-Selective Cortex." *Journal of Neuroscience* 42, no. 39 (September 28, 2022): 7412–30. <https://doi.org/10.1523/JNEUROSCI.1894-21.2022>.

- Shain, Cory, Hope Kean, Colton Casto, Benjamin Lipkin, Josef Affourtit, Matthew Siegelman, Francis Mollica, and Evelina Fedorenko. "Distributed Sensitivity to Syntax and Semantics throughout the Language Network." *Journal of Cognitive Neuroscience* 36, no. 7 (June 1, 2024): 1427–71. https://doi.org/10.1162/jocn_a_02164.
- Shashidhara, Sneha, Moataz Assem, Matthew F Glasser, and John Duncan. "Task and Stimulus Coding in the Multiple-Demand Network." *Cerebral Cortex* 34, no. 7 (July 1, 2024): bhae278. <https://doi.org/10.1093/cercor/bhae278>.
- Shashidhara, Sneha, and Yaara Erez. "Reward Motivation Increases Univariate Activity but Has Limited Effect on Coding of Task-Relevant Information across the Frontoparietal Cortex." *Neuropsychologia* 160 (September 17, 2021): 107981. <https://doi.org/10.1016/j.neuropsychologia.2021.107981>.
- Shashidhara, Sneha, Daniel J. Mitchell, Yaara Erez, and John Duncan. "Progressive Recruitment of the Frontoparietal Multiple-Demand System with Increased Task Complexity, Time Pressure, and Reward." *Journal of Cognitive Neuroscience* 31, no. 11 (November 2019): 1617–30. https://doi.org/10.1162/jocn_a_01440.
- Shashidhara, Sneha, Floortje S. Spronkers, and Yaara Erez. "Individual-Subject Functional Localization Increases Univariate Activation but Not Multivariate Pattern Discriminability in the 'Multiple-Demand' Frontoparietal Network." *Journal of Cognitive Neuroscience* 32, no. 7 (July 1, 2020): 1348–68. https://doi.org/10.1162/jocn_a_01554.
- Skordos, Dimitrios, Ann Bunger, Catherine Richards, Stathis Selimis, John Trueswell, and Anna Papafragou. "Motion Verbs and Memory for Motion Events." *Cognitive Neuropsychology* 37, no. 5–6 (August 17, 2020): 254–70. <https://doi.org/10.1080/02643294.2019.1685480>.
- Smith, Kevin A., and Edward Vul. "Sources of Uncertainty in Intuitive Physics." *Topics in Cognitive Science* 5, no. 1 (January 2013): 185–99. <https://doi.org/10.1111/tops.12009>.
- Spelke, Elizabeth. *What Babies Know: Core Knowledge and Composition: Volume 1*. Oxford Cognitive Development Series. New York: Oxford University Press, 2022.
- Spelke, Elizabeth S., and Katherine D. Kinzler. "Core Knowledge." *Developmental Science* 10, no. 1 (January 2007): 89–96. <https://doi.org/10.1111/j.1467-7687.2007.00569.x>.
- Tuckute, Greta, Aalok Sathe, Shashank Srikant, Maya Taliaferro, Mingye Wang, Martin Schrimpf, Kendrick Kay, and Evelina Fedorenko. "Driving and Suppressing the Human Language Network Using Large Language Models." *Nature Human Behaviour* 8, no. 3 (January 3, 2024): 544–61. <https://doi.org/10.1038/s41562-023-01783-7>.
- Tversky, Amos, and Daniel Kahneman. "The Framing of Decisions and the Psychology of Choice." *Science* 211, no. 4481 (1981): 453–58. <https://doi.org/10.1126/science.7455683>.
- Varley, Rosemary A., Nicolai J. C. Klessinger, Charles A. J. Romanowski, and Michael Siegal. "Agrammatic but Numerate." *Proceedings of the National Academy of Sciences* 102, no. 9 (March 2005): 3519–24. <https://doi.org/10.1073/pnas.0407470102>.
- Varley, Rosemary, and Michael Siegal. "Evidence for Cognition without Grammar from Causal Reasoning and 'Theory of Mind' in an Agrammatic Aphasic Patient." *Current Biology* 10, no. 12 (June 2000): 723–26. [https://doi.org/10.1016/S0960-9822\(00\)00538-8](https://doi.org/10.1016/S0960-9822(00)00538-8).
- Vurgun, Uğurcan, Yue Ji, and Anna Papafragou. "Aspectual Processing Shifts Visual Event Apprehension." *Cognitive Science* 48, no. 6 (2024): e13476. <https://doi.org/10.1111/cogs.13476>.
- Vurgun, Ugurcan, Yue Ji, and Anna Papafragou. "Linguistic Aspect Constrains Event Apprehension." *Proceedings of the Annual Meeting of the Cognitive Science Society* 44, no. 44 (2022). <https://escholarship.org/uc/item/2d17k1nw>.

- 1
2
3
4 Willems, Roel M., Lise Van Der Haegen, Simon E. Fisher, and Clyde Francks. "On the Other
5 Hand: Including Left-Handers in Cognitive Neuroscience and Neurogenetics." *Nature*
6 *Reviews Neuroscience* 15, no. 3 (March 2014): 193–201. <https://doi.org/10.1038/nrn3679>.
7
8 Wolna, Agata, Jakub Szewczyk, Michele Diaz, Aleksandra Domagalik, Marcin Szwed, and
9 Zofia Wodniecka. "Tracking Components of Bilingual Language Control in Speech
10 Production: An fMRI Study Using Functional Localizers." *Neurobiology of Language* 5, no.
11 2 (June 3, 2024): 315–40. https://doi.org/10.1162/nol_a_00128.
12
13 Wong, Lionel, Gabriel Grand, Alexander K. Lew, Noah D. Goodman, Vikash K. Mansinghka,
14 Jacob Andreas, and Joshua B. Tenenbaum. "From Word Models to World Models:
15 Translating from Natural Language to the Probabilistic Language of Thought." arXiv, June
16 23, 2023. <https://doi.org/10.48550/arXiv.2306.12672>.
17
18 Woolgar, Alex, John Duncan, Facundo Manes, and Evelina Fedorenko. "The Multiple-Demand
19 System but Not the Language System Supports Fluid Intelligence." *Nature Human*
20 *Behaviour* 2, no. 3 (March 2018): 200–204. <https://doi.org/10.1038/s41562-017-0282-3>.
21
22 Xu, Fei. "Towards a Rational Constructivist Theory of Cognitive Development." *Psychological*
23 *Review* 126, no. 6 (November 2019): 841–64. <https://doi.org/10.1037/rev0000153>.
24
25 Xu, Rui, Narcisse P. Bichot, Atsushi Takahashi, and Robert Desimone. "The Cortical
26 Connectome of Primate Lateral Prefrontal Cortex." *Neuron* 110, no. 2 (January 2022): 312–
27 327.e7. <https://doi.org/10.1016/j.neuron.2021.10.018>.
- 28
29
30
31
32
33
34
35
36
37
38
39
40
41
42
43
44
45
46
47
48
49
50
51
52
53
54
55
56
57
58
59
60
61
62
63
64
65